

## Engineering design earthquakes from multimodal hazard disaggregation

Iunio Iervolino<sup>a,\*</sup>, Eugenio Chioccarelli<sup>a</sup>, Vincenzo Convertito<sup>b</sup>

<sup>a</sup> Dipartimento di Ingegneria Strutturale, Università degli Studi di Napoli Federico II, Via Claudio 21, 80125 Naples, Italy

<sup>b</sup> Istituto Nazionale di Geofisica e Vulcanologia, Osservatorio Vesuviano, Naples, Italy

### ARTICLE INFO

#### Article history:

Received 20 December 2010

Received in revised form

6 April 2011

Accepted 1 May 2011

Available online 23 May 2011

### ABSTRACT

To define reference structural actions, engineers practicing earthquake resistant design are required by codes to account for ground motion likely to threaten the site of interest and also for pertinent seismic source features. In most of the cases, while the former issue is addressed assigning a mandatory design response spectrum, the latter is left unsolved. However, in the case that the design spectrum is derived from probabilistic seismic hazard analysis, disaggregation may be helpful, allowing to identify the earthquakes having the largest contribution to the hazard for the spectral ordinates of interest. Such information may also be useful to engineers in better defining the design scenario for the structure, e.g., in record selection for nonlinear seismic structural analysis. On the other hand, disaggregation results change with the spectral ordinate and return period, and more than a single event may dominate the hazard, especially if multiple sources affect the hazard at the site. This work discusses identification of engineering design earthquakes referring, as an example, to the Italian case. The considered hazard refers to the exceedance of peak ground acceleration and 1s spectral acceleration with four return periods between 50 and 2475 year. It is discussed how, for most of the Italian sites, more than a design earthquake exists, because of the modeling of seismic sources. Furthermore, it is explained how and why these change with the limit state and the dynamic properties of the structure. Finally, it is illustrated how these concepts may be easily included in engineering practice complementing design hazard maps and effectively enhancing definition of design seismic actions with relatively small effort.

© 2011 Elsevier Ltd. All rights reserved.

### 1. Introduction

Earthquake resistant design in international seismic codes relies widely on a target spectrum to define seismic actions on structures. Being a synthetic representation of ground motion, the design spectrum should implicitly include information about the features of the seismogenetic sources determining the seismic hazard at the construction site. Nevertheless, prudently, the practitioner is often required to also account explicitly for them, for example, when dealing with ground motion record selection as an input for the nonlinear seismic structural analyses (e.g., [1,2]). For example, Eurocode 8 [3], or EC8, provides that: *In the range of periods between  $0.2T_1$  and  $2T_1$ , where  $T_1$  is the fundamental period of the structure in the direction where the accelerogram will be applied, no value of the mean 5% damping elastic spectrum, calculated from all time histories, should be less than 90% of the corresponding value of the 5% damping elastic response spectrum.* Moreover, accelerograms should be *adequately qualified with regard to the seismogenetic features of the sources* [...].

In most of the cases, it is unlikely that the engineer has the information and/or is able to qualify the input ground motions with respect to the seismological features of the seismic sources.<sup>1</sup> However, if the design spectrum is related to probabilistic seismic hazard analysis (PSHA), it is possible to obtain *design earthquakes* (DEs) in terms of magnitude, location and other parameters such as faulting style, hanging/foot wall, etc.

In fact, PSHA allows one to compute the average return period of ground motions exceeding a given intensity measure (*IM*) threshold at the considered site [4]. On the other hand, if the return period of seismic action for design purposes is defined *a priori*, and if the *IM* is the elastic spectral acceleration at different structural periods, it is possible to build the uniform hazard spectrum (UHS), i.e., the response spectrum with a constant exceedance probability for all ordinates, e.g., 10% in 50 year (or, equivalently, 475 yr return period) in the case of design for life-safety structural performance [5]. UHS is not the only possible PSHA-based design spectrum [6], but it is, to

<sup>1</sup> EC8 actually requires information about seismic source also in choosing between two possible design spectrum shapes stating that: *If the earthquakes that contribute most to the seismic hazard defined for the site for the purpose of probabilistic hazard assessment have a surface-wave magnitude,  $M_s$ , not greater than 5.5, it is recommended that the Type 2 spectrum is adopted.*

\* Corresponding author. Tel.: +39 0817683488; fax: +39 0817685921.  
E-mail address: [iunio.iervolino@unina.it](mailto:iunio.iervolino@unina.it) (I. Iervolino).

date, the basis for the definition of design seismic actions on structures in the most advanced seismic codes. In fact, the Italian seismic code [7] is based on the work of the *Istituto Nazionale di Geofisica e Vulcanologia* (INGV), which computed uniform hazard spectra over a grid of more than 10,000 points for 9 return periods ( $T_r$ ) from 30 to 2475 yr, and 10 spectral ordinates from 0.1 to 2 s (<http://esse1.mi.ingv.it/>). As a consequence, at each site, Italian design spectra are a close approximation of the UHS.

If UHS is the design spectrum, *disaggregation* of seismic hazard [8] identifies the values of some earthquake characteristics providing the largest contributions to the hazard in terms of exceeding a specified spectral ordinate threshold. These events may be referred to as the earthquakes dominating the seismic hazard in a probabilistic sense, and may be used as DEs, as conceptually introduced by McGuire [4]. In a previous work (i.e., [9]) the authors elaborated on this topic referring to a case-study region in southern Italy. Herein, the issues raised about identification of DEs are investigated further and taken to a national level. This is relevant because modern codes increasingly rely on PSHA to define the design spectra yet giving limited, if any, information about the design scenarios. It may be useful, then, to develop tools complementary to design spectra and hazard maps, and based on disaggregation, which allow the practitioner to identify the scenario seismic events of interest (e.g., maps of DEs), as also invoked by Bommer [10].

In the present study DEs are identified disaggregating the probabilistic seismic hazard, computed for two spectral ordinates intended to represent the short and moderate period portions of the response spectrum, and four return periods. Disaggregation is expressed in terms of magnitude ( $M$ ), source to site distance ( $R$ ) and  $\varepsilon$  (the number of standard deviations that the ground motion  $IM$  is away from its median value estimated by the assumed attenuation relationship).

Along with mapping of design events, it is shown first that, for most Italian sites, two DEs exist, a moderate-close one and a strong-distant one, and it is explained why this depends on the modeling of seismic sources considered in PSHA. Second, results of the study include discussion of how and why DEs change with the spectral ordinate (i.e., the dynamic characteristics of the considered structure), the return period of the seismic action and with relative distance to seismogenic zones. It is also demonstrated why, although it may sound counterintuitive [9], the contribution of the moderate-close event increases with the return period with respect to the strong-distant earthquake. Finally, it is illustrated how maps of DEs may be easy yet useful complements to design acceleration maps for both ordinary and advanced engineering practices.

## 2. Methodology

Given a seismic source model and a ground-motion prediction equation (GMPE), PSHA provides, for a selected site, the hazard curve representing the mean annual frequency of exceedance of a ground motion  $IM$ . Starting from the PSHA results, disaggregation is a procedure that allows identification of the hazard contribution of each  $\{M, R, \varepsilon\}$  vector. The analytical result of disaggregation is the joint probability density function<sup>2</sup> (PDF) of  $\{M, R, \varepsilon\}$  conditional to the exceedance of an  $IM$  threshold ( $IM_0$ ):

$$f(m, r, \varepsilon | IM > IM_0) = \frac{\sum_{i=1}^n v_i \cdot I[IM > IM_0 | m, r, \varepsilon] \cdot f(m, r, \varepsilon)}{\lambda_{IM_0}} \quad (1)$$

<sup>2</sup> In principle other source features may be considered in disaggregation (e.g., faulting style, hanging/foot wall, etc.) yet their relevance with respect to engineering practice is not fully proven to date.

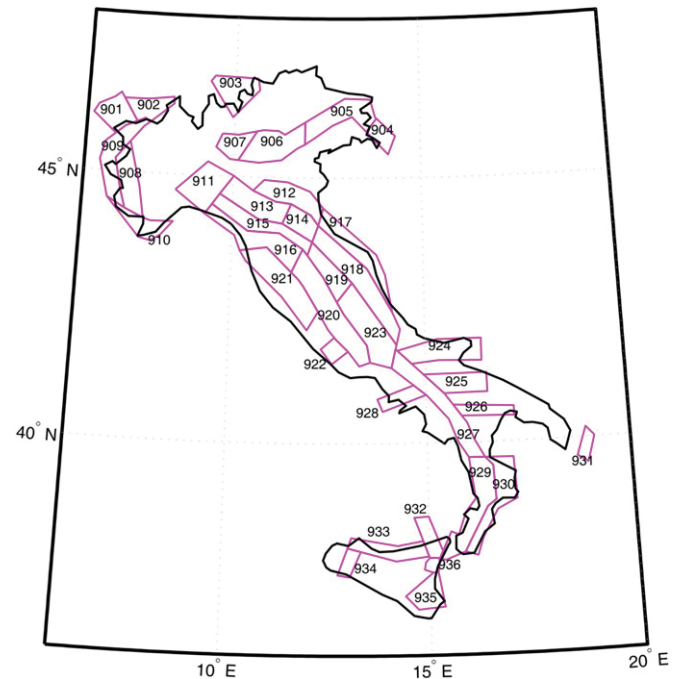


Fig. 1. Seismogenic zones for Italy according to [11].

In Eq. (1)  $I$  is an indicator function that is equal to 1 if  $IM$  is larger than  $IM_0$  for a given distance  $r$ , magnitude  $m$  and  $\varepsilon$ ;  $n$  is the number of seismic sources relevant for the hazard at the site;  $v_i$  is the earthquake occurrence probability for the fault  $i$ ;  $f(m, r, \varepsilon)$  is the joint PDF of  $\{M, R, \varepsilon\}$  and  $\lambda_{IM_0}$  is the hazard for  $IM_0$ .

Because disaggregation results may change with the considered spectral period, in this work DEs are computed for two different spectral accelerations,<sup>3</sup>  $S_a$ , at 0 s (i.e., peak ground acceleration or PGA) and 1 s in order to account for short and moderate period regions of the response spectrum.

To perform disaggregation it is required first to compute hazard for the two  $IM$ s considered. Both PSHA and disaggregation analyses were performed by a computer program specifically developed and also used in [9]. The whole country was discretized using the same grid of about 10,760 points adopted by INGV and, therefore, by the Italian seismic code. The seismogenic sources are that of [11], adopted by INGV (Fig. 1), while seismic parameters of each zone are those used by Barani et al. [12],<sup>4</sup> as given in Table 1.

According to Ambraseys et al. [14], which is the GMPE considered: magnitude is that of surface waves ( $M_s$ ). All the analyses refer to rock or stiff soil conditions.

Assuming a uniform epicenter distribution in each seismogenic zone, epicentral distance distribution is the appropriate one. Because the used GMPE refers to the closest horizontal distance to the surface projection of the fault plane ( $R_{jb}$ ) as defined by Joyner and Boore [15], the former was converted into the latter via the linear relationship given in [16]. Distance applicability limits of the GMPE were respected and contributions to hazard distant more than 200 km from the site were neglected in computations, which considered four return periods corresponding to the reference limit

<sup>3</sup> INGV also indirectly provides data about the seismic scenarios mostly contributing to the hazard, but only referring to peak ground acceleration.

<sup>4</sup> An erratum [13] to this reference reports  $b$  values for zones 903, 920 and 922 different with respect to those considered in this study. However, given the differences between correct and incorrect values and geographical location of zones, it is believed that changing these parameters should have minor influence on the results presented in the following.

**Table 1**

Characterization of seismic sources according to Barani et al. [12]. For each zone the following is provided: minimum ( $M_{min}$ ) and maximum magnitude ( $M_{max}$ ); annual rate of earthquake occurrence above  $M_{min}$ , ( $\nu$ ) and negative slope of the Gutenberg–Richter relationship ( $b$ ).

Zone	$M_{min}$	$M_{max}$	$\nu$	$b$
901	4.3	5.8	0.045	1.133
902	4.3	6.1	0.103	0.935
903	4.3	5.8	0.117	1.786
904	4.3	5.5	0.050	0.939
905	4.3	6.6	0.316	0.853
906	4.3	6.6	0.135	1.092
907	4.3	5.8	0.065	1.396
908	4.3	5.5	0.140	1.408
909	4.3	5.5	0.055	0.972
910	4.3	6.4	0.085	0.788
911	4.3	5.5	0.050	1.242
912	4.3	6.1	0.091	1.004
913	4.3	5.8	0.204	1.204
914	4.3	5.8	0.183	1.093
915	4.3	6.6	0.311	1.083
916	4.3	5.5	0.089	1.503
917	4.3	6.1	0.121	0.794
918	4.3	6.4	0.217	0.840
919	4.3	6.4	0.242	0.875
920	4.3	5.5	0.317	1.676
921	4.3	5.8	0.298	1.409
922	4.3	5.2	0.090	1.436
923	4.3	7.3	0.645	0.802
924	4.3	7.0	0.192	0.945
925	4.3	7.0	0.071	0.508
926	4.3	5.8	0.061	1.017
927	4.3	7.3	0.362	0.557
928	4.3	5.8	0.054	1.056
929	4.3	7.6	0.394	0.676
930	4.3	6.6	0.146	0.715
931	4.3	7.0	0.045	0.490
932	4.3	6.1	0.118	0.847
933	4.3	6.1	0.172	1.160
934	4.3	6.1	0.043	0.778
935	4.3	7.6	0.090	0.609
936	3.7	5.2	0.448	1.219

states for civil and strategic structures (i.e., 50, 475, 975 and 2475 yr).

It is also to mention that no background seismicity was included; this is consistent with the INGV assumptions, as no significant influence on hazard was found; see [17] for details.

### 2.1. PGA and Sa(1 s) hazards

Hazard curves were computed using thirty values of the  $IM$ s equally distributed between 0.001 and 1.5g. Computed hazard maps for the two spectral ordinates and the four return periods are reported in Figs. 2 and 3. In order to validate these results INGV data are assumed to be the benchmark, and with respect to them the hazard values computed in this study are in good general agreement. In fact, INGV considered an extended logic-tree accounting for two earthquake catalogs, two different seismic rate models and maximum magnitude estimations and four attenuation models [17]. This explains some differences found: in particular PGA differs from INGV mostly for sites enclosed into zones 927 and 935, while Sa(1 s) for zones 905 and 935 (refer to <http://esse1.mi.ingv.it/> for comparisons).

Discrepancies derive mostly from the mentioned different hazard modelings, but analyzing the results for sites in zones 905, a non-negligible influence of the lumping of hazard curves in a certain number of  $IM$  values was also found. In fact, on computing PSHA again and assuming a finer discretization (60 points equally distributed between 0.001 and 1.5g), accordance with INGV results is significantly improved; however, choice of thirty points was

retained as a compromise that seems to provide trends of results that are generally acceptable and affordable for computing time demand.

Because the main object of the work is the definition of DEs, accordance with INGV disaggregation data was considered more important than that related to hazard data. Validation refers to PGA (disaggregation of Sa(1 s) is not provided by INGV) and, again, general consistency was found; some exceptions were identified for some low seismicity sites (also in this case increasing  $IM$  discretization may reduce the gap). While details cannot be reported here for the sake of brevity, the reader is referred to Chioccarelli [18] for further information.

### 3. Identifying and mapping design earthquakes

Disaggregation integral in Eq. (1) is computed numerically by the software using bins of 0.05, 1.0 km and 0.5 for  $M$ ,  $R$  and  $\varepsilon$ , respectively, ( $\varepsilon$  varies between  $-3$  and  $+3$ ). This means that the disaggregation PDF, which is continuous in principle, is rendered a discrete function.

Recalling that for each site, return period and spectral ordinate, disaggregation results in a four-dimensional surface providing the contribution to hazard of  $M$ ,  $R$  and  $\varepsilon$  variables, multiple DEs can be identified. Herein, the *first* DE is defined as the mode of the disaggregation PDF, i.e., the vector  $\{M^*, R^*, \varepsilon^*\}$  most frequently causing the exceedance of the  $IM$  threshold corresponding to the considered return period. Moreover, as extensively discussed in [9], because analyses show that in many cases disaggregation PDF has more than a single mode significantly contributing to hazard, a *second* DE is defined as the second relative maximum of the  $f(m, r, \varepsilon | IM > IM_0)$  distribution. Herein, to ensure the second DE to be of practical relevance, two additional (arbitrary) conditions were imposed with respect to [9]:

1. the second mode is identified as an event different from the first DE if the two differ by 5.0 km in distance and/or 0.25 in magnitude and
2. the second DE is considered as such if the second mode of the disaggregation PDF gives a contribution to hazard larger than  $10^{-4}$ .

See next section for the analysis of significance of DEs identified via these criteria.

Maps of DEs are reported in Figs. 4–11 ( $R$  in km), in which it is possible to identify some general trends: (i) the first mode corresponds to an earthquake caused by the closer source (or the source the site is enclosed into) and with low-to-moderate magnitude, (ii) the second mode accounts for the influence of the more distant zones usually with larger magnitude and (iii) moving from PGA to Sa, the number of sites with two DEs increases. As a consequence of (ii) and (iii), it can be inferred that the influence of more distant zones is higher for Sa(1 s) than for PGA.

Each of these conclusions will be examined further and explained in the following via the case studies referring to specific sites. It may be anticipated that, of course, all disaggregation results can be motivated looking at GMPE and seismogenic model adopted. However, because most of the ordinary GMPEs show similar dependencies with respect to magnitude and distance, while several different options may underlie modeling of seismic sources, it is believed that changing GMPE may change the results without losing general trends, conversely, changing the seismic source model (especially the geometrical shape of source zones) can alter results dramatically.

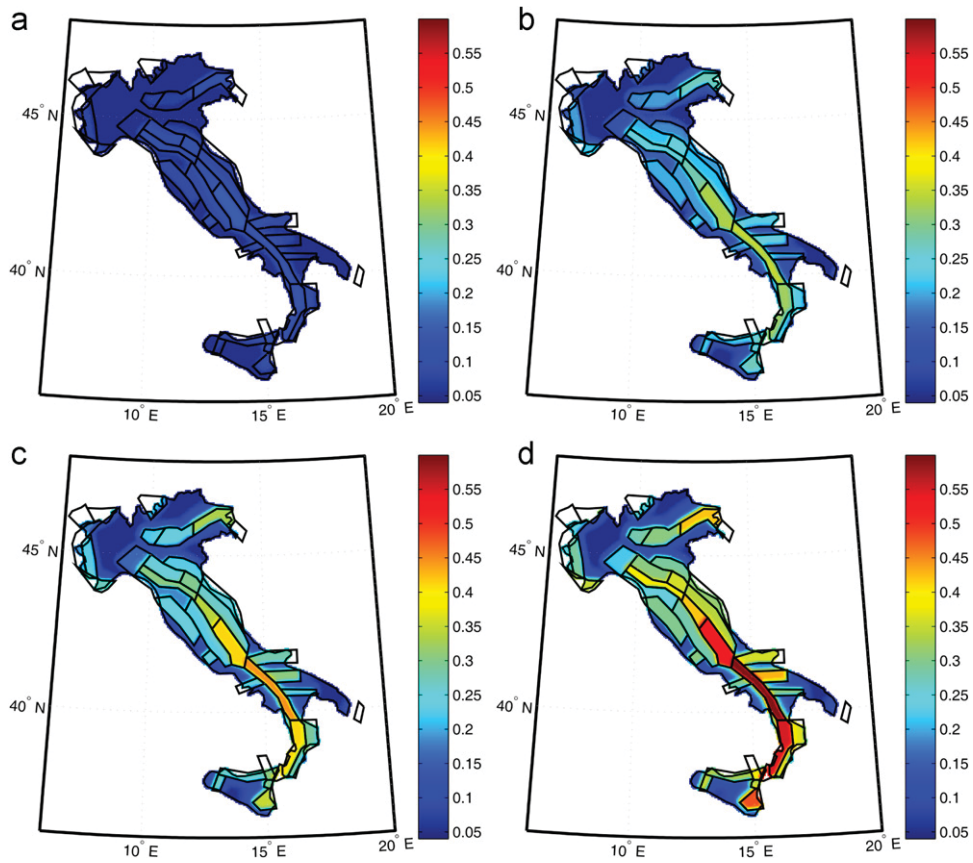


Fig. 2. Hazard maps of PGA, in fractions of  $g$ , for  $T_r$  equal to 50 yr (a), 475 yr (b), 975 yr (c) and 2475 yr (d).

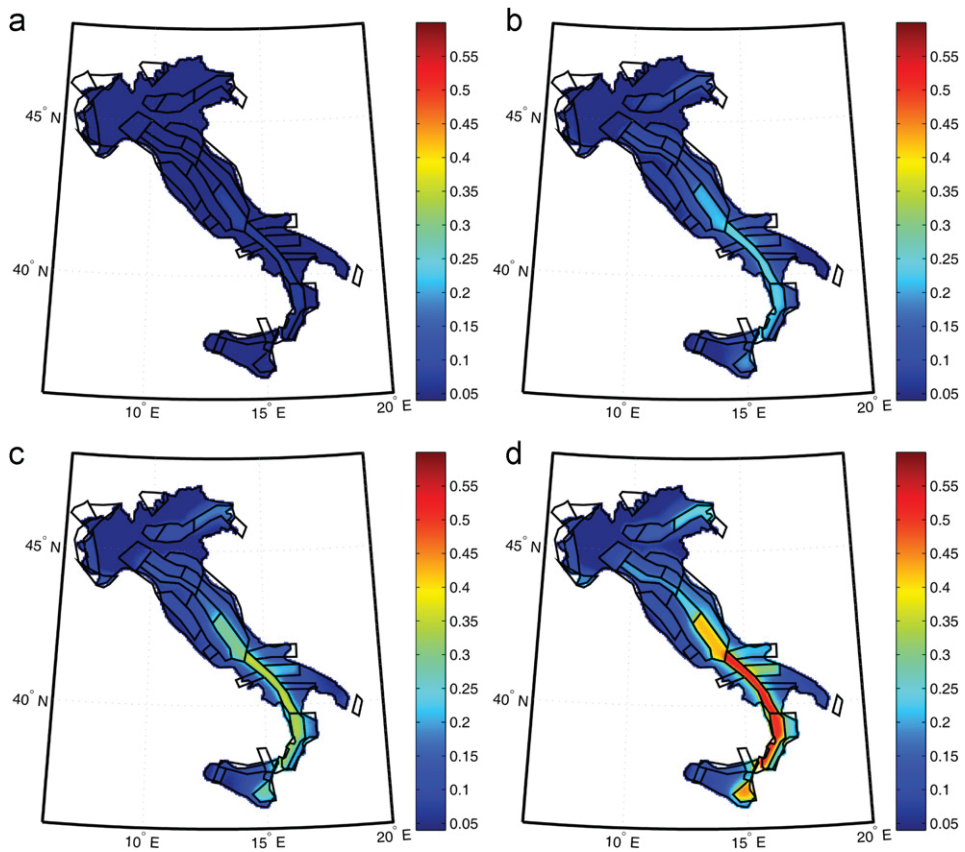


Fig. 3. Hazard maps of  $S_a(1\text{ s})$ , in fractions of  $g$ , for  $T_r$  equal to 50 yr (a), 475 yr (b), 975 yr (c) and 2475 yr (d).

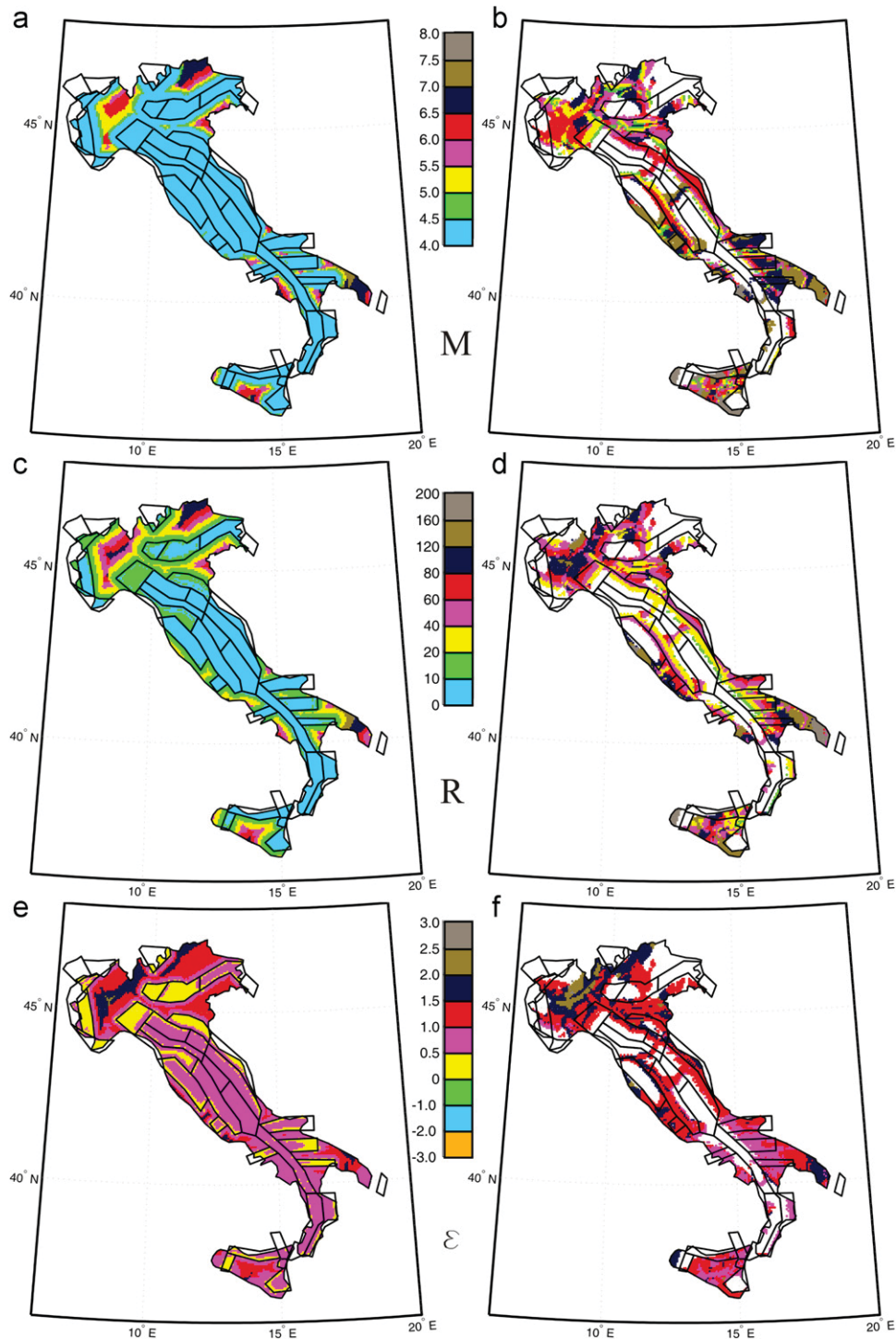


Fig. 4. First (left) and second (right) modal values for PGA and  $T_r=50$  yr.

### 3.1. Implications of disaggregation modes as design scenarios

#### 3.1.1. Significance based on contributions to hazard

Identification of DEs by modal values, as shown in the maps above, is useful for the practical use of disaggregation results. However, in some cases they cannot be representative enough of the whole disaggregation distribution. Examples of critical cases are reported below while in the next sections specific sites are studied.

Because many different earthquakes can affect the hazard at a site, disaggregation may show an especially flat shape. When this condition occurs, modal values can be comparatively less

representative to determine design scenarios. An example is the site of Campobasso ( $14.668^\circ\text{E}$ ,  $41.561^\circ\text{N}$ ) considered here for  $S_a(1\text{ s})$  and  $T_r$  equal to 50 yr. Location and disaggregation distribution<sup>5</sup> are shown in Fig. 12 (hereafter, considered sites are indicated in the maps by triangles). According to the procedure described in

<sup>5</sup> Hereafter for all the site-specific cases, disaggregation surfaces will be shown as tridimensional, i.e., after marginalization of  $f(m,r,\varepsilon|IM > IM_0)$  with respect to  $\varepsilon$  so to obtain  $f(m,r|IM > IM_0) = \int_{\varepsilon} f(m,r,\varepsilon|IM > IM_0)d\varepsilon$ . Despite this pictorial choice, modal values presented are always computed on the four-dimensional disaggregation surface.

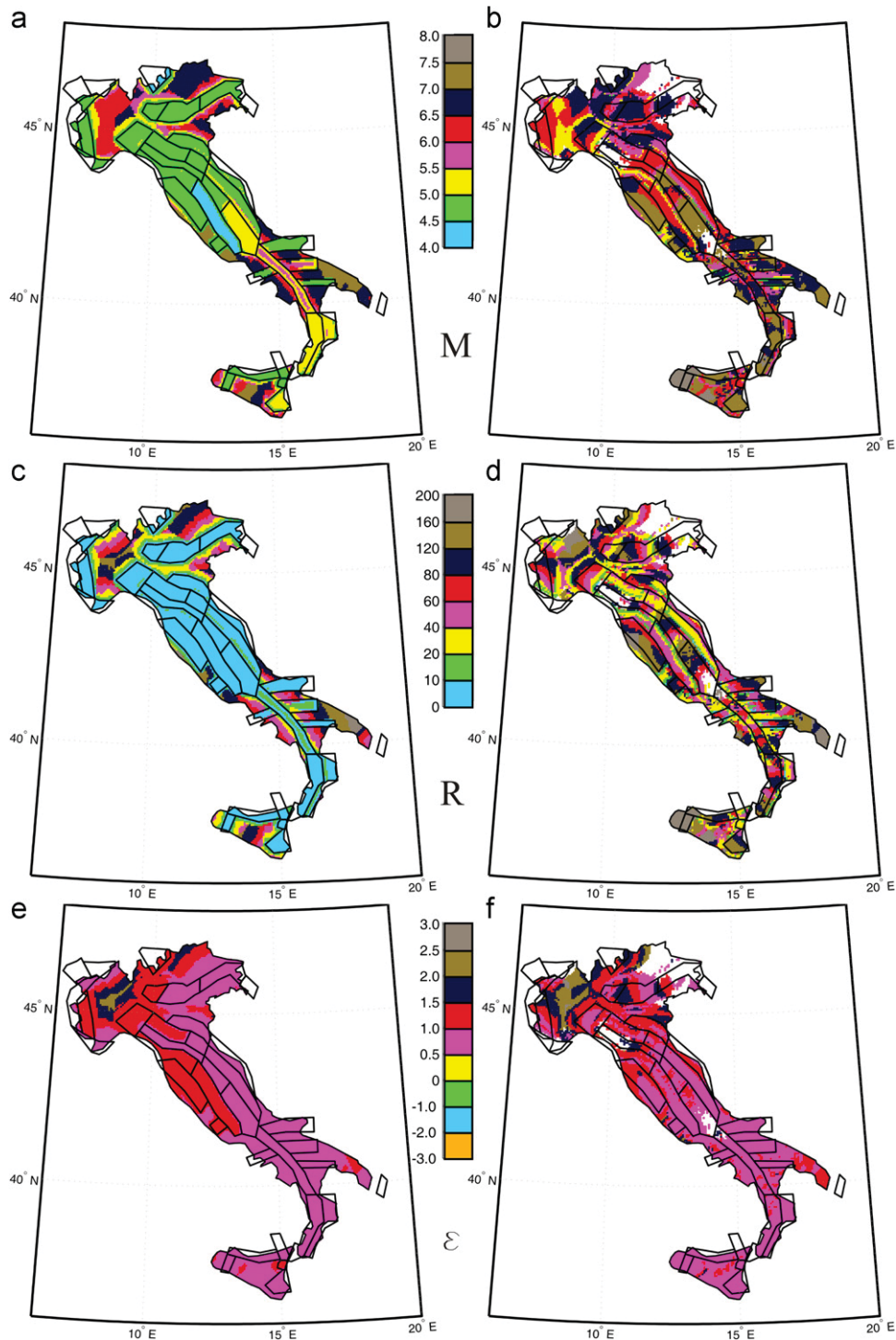


Fig. 5. First (left) and second (right) modal values for  $S_a(1\text{ s})$  and  $T_r=50\text{ yr}$ .

the previous section, the first and the second DEs are  $\{6.5\text{ km}, 4.93, 0.5\}$  and  $\{13.5\text{ km}, 5.53, 0.5\}$ , respectively, in terms of distance, magnitude and  $\varepsilon$  and the distribution does not seem to have a third significant mode but it is clear that large distance and magnitude values also give a non-negligible hazard contribution.

Referring to identification of the second mode, the  $10^{-4}$  minimum contribution threshold has been chosen looking at disaggregation for several sites, yet it is still arbitrary and PDFs can have different shapes in a way that a unique assumption may not satisfy all the cases. As a site-specific example, the Caltanissetta city ( $14.18^\circ\text{E}$ ,  $37.33^\circ\text{N}$ ) is considered. The disaggregation of

$T_r=50\text{ yr}$  PGA hazard for this location is reported in Fig. 13a. The first and the second DEs are identified in terms of  $R$  and  $M$  as  $\{54.5\text{ km}, 6.08, 1.0\}$  and  $\{144.5\text{ km}, 7.58, 1.0\}$ , while associated probabilities are  $5.6 \times 10^{-3}$  and  $5.7 \times 10^{-4}$ , respectively. Considering a second DE, it seems to be a reasonable choice because several  $M$  and  $R$  bins give low but non-negligible contribution to hazard in a way that globally the second mode appears significant.<sup>6</sup>

<sup>6</sup> Importance of magnitude and distance for engineering practice may refer, for example, to cyclic demand imposed to structures by ground motion,

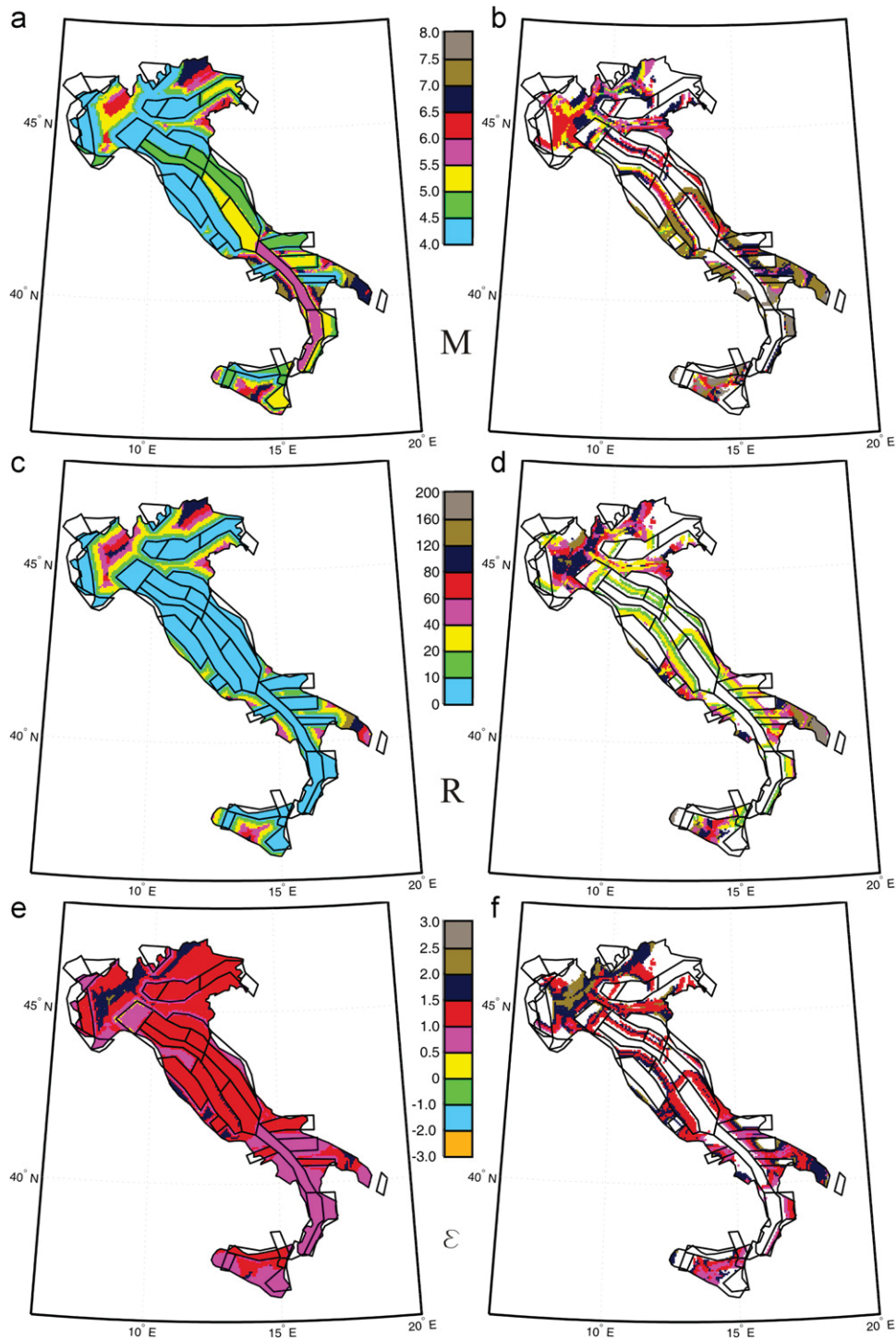


Fig. 6. First (left) and second (right) modal values for PGA and  $T_r=475$  yr.

Conversely, looking at disaggregation for  $T_r=475$  yr PGA hazard in Naples ( $14.191^\circ\text{E}$ ,  $40.829^\circ\text{N}$ ), Fig. 13b, the second mode  $\{50.5 \text{ km}$ ,  $7.3$ ,  $1.50\}$  has an hazard contribution<sup>7</sup> equal to  $2.8 \times 10^{-4}$ , but its contribution seems to be negligible because no other close bins have comparable associated probability.

(footnote continued)

i.e., different earthquakes determining similar spectral ordinate may be different in duration if characterized by different  $M$  and  $R$  pairs [19].

<sup>7</sup> In the plots, bins with contribution lower than  $1.2 \times 10^{-3}$  are shown in white.

### 3.1.2. Significance based on spectral regions

Disaggregation of 1 s spectral acceleration was considered representative of a response spectrum region of engineering interest. In fact, in this section hazard disaggregation for other structural periods is shown to assess the range in which 1 s results can still be considered significant. The analyzed site is Viterbo ( $12.107^\circ\text{E}$ ,  $42.426^\circ\text{N}$ ). In Figs. 14 and 15 PDFs for  $T_r=50$  and 2475 yr are reported. For both return periods disaggregation for spectral acceleration at 4 structural periods is given: PGA, 0.5, 1 and 2 s.

For  $T_r=50$  yr, it appears, as expected, that results for  $T=2$  s are well represented by disaggregation for  $T=1$  s, much better if

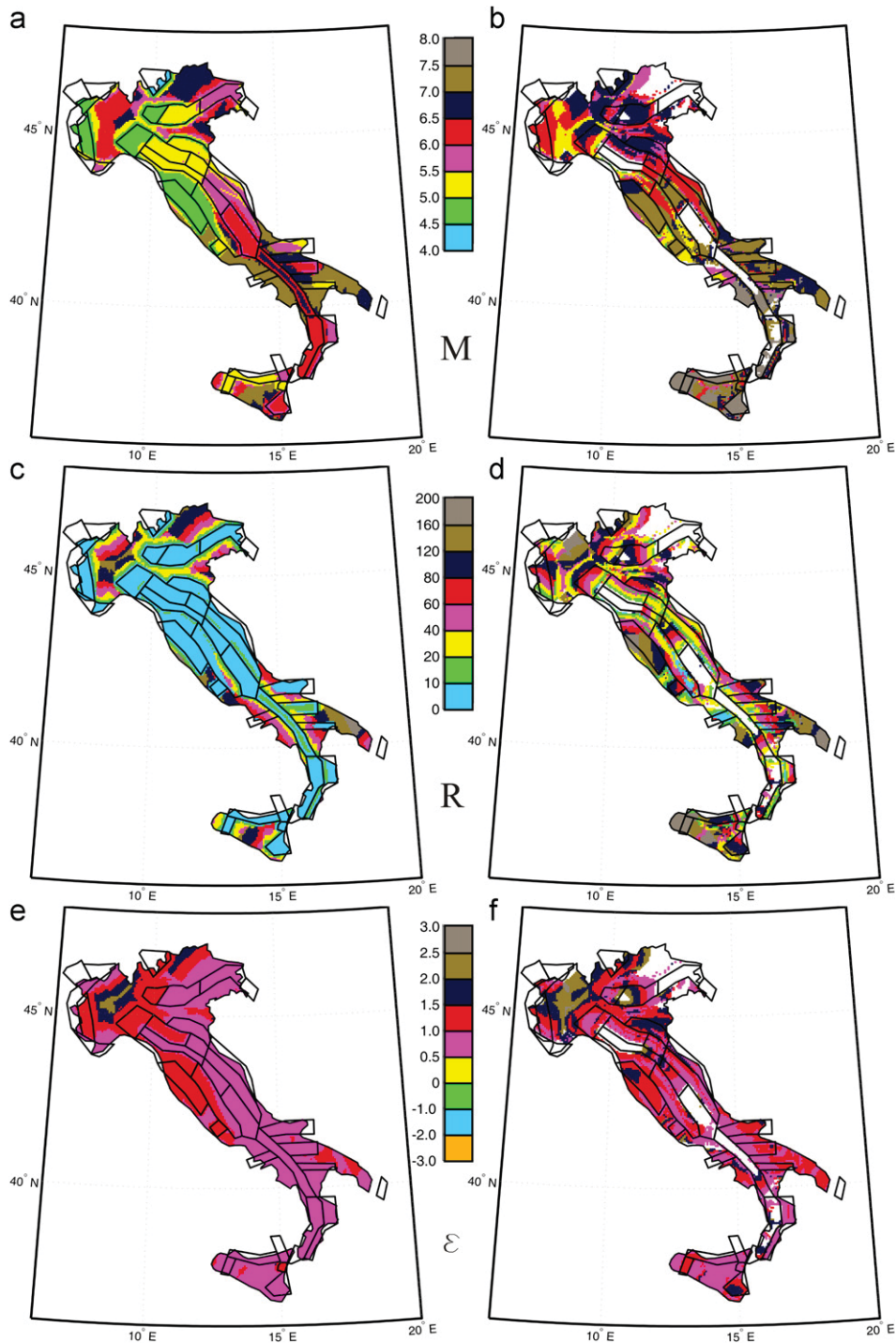


Fig. 7. First (left) and second (right) modal values for  $S_a(1\text{ s})$  and  $T_r=475\text{ yr}$ .

compared to PGA. Also disaggregation for  $T=0.5\text{ s}$  seems to be better represented by  $T=1\text{ s}$  results with respect to PGA, because of a second mode more clearly appearing in the latter with respect to the former.

Although less evident, the same conclusion holds for  $T_r=2475\text{ yr}$  because the contribution of the second mode (evident for  $T=1\text{ s}$ ) is also visible for  $T=0.5\text{ s}$ . In particular, the second DE is  $\{67.5\text{ km}, 7.28, 1.5\}$  and gives a contribution to hazard equal to  $1.2 \times 10^{-3}$ , which is significant according to the threshold conventionally established in the previous section. Therefore, disaggregation of PGA hazard seems representative for structures with fundamental period below  $0.5\text{ s}$ . In all other cases, disaggregation for  $S_a(1\text{ s})$  is a more rational choice.

It is to note, finally, how contribution to hazard of second mode increases, if disaggregation is for a spectral ordinate corresponding to a longer period; this is systematic and explained in Section 4.1.

#### 4. One, two or more modes?

From the DE maps given above, it appears that the second mode of disaggregation PDFs is not always identified (white regions in the maps) and that disaggregation is unimodal within, or around, specific seismic source zones. In fact, if a site is enclosed or close to a seismic

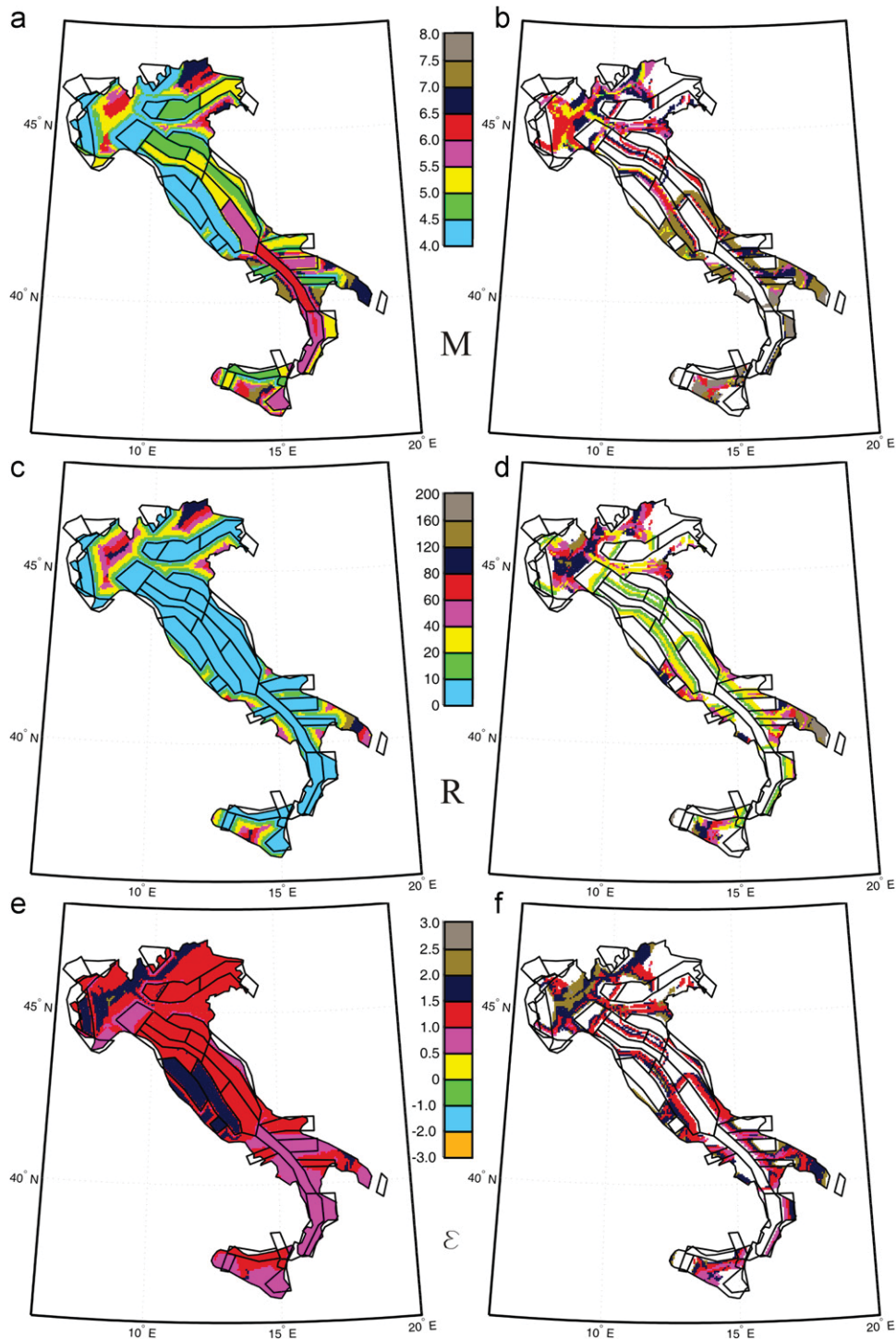


Fig. 8. First (left) and second (right) modal values for PGA and  $T_r=975$  yr.

source zone with *high seismicity* (in terms of a combination of magnitude interval, annual rate of earthquake and *b*-value of Gutenberg–Richter) with respect to the surrounding zones, the stronger zone dominates the hazard for the site. As a consequence, contributions to hazard will be concentrated in a relatively narrow *M* and *R* domain whose limits generally correspond to the minimum and maximum values of magnitude and distance of the zone borders from the site. For these cases, given the return period and the spectral ordinate of interest, the disaggregation PDF is unimodal and, therefore, characterized by a single DE.

One of these sites is represented by L'Aquila (13.396°E, 42.365°N) whose disaggregation is reported here for a return period equal to 975 yr (Fig. 16) along with zones considered in its hazard computation. The site is enclosed in zone 923 characterized by  $M_{max}$  equal to 7.3, annual rate of earthquake occurrence ( $\nu$ ) equal to 0.645 and a *b*-value of 0.802 (Table 1). All the closer zones (918, 919, 920) have lower maximum magnitude, lower  $\nu$  and higher *b*. These numbers suggest that zone 923 has the higher seismicity and, therefore, unimodal disaggregation is expected, as shown.

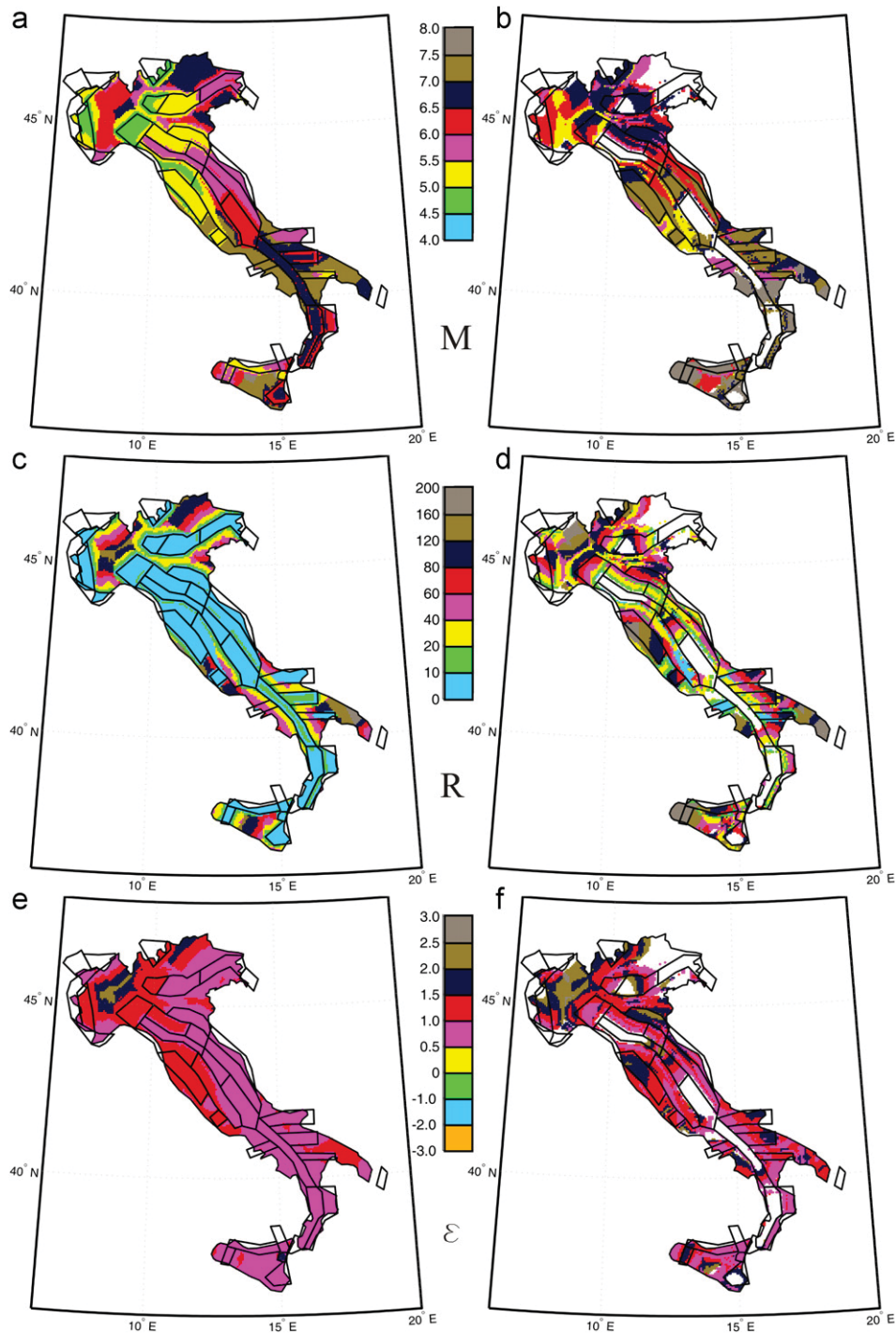


Fig. 9. First (left) and second (right) modal values for  $S_a(1\text{ s})$  and  $T_r=975\text{ yr}$ .

Conversely, maps indicate at least two different DEs for many sites. An example is the city of Bari ( $16.879^\circ\text{E}$ ,  $41.113^\circ\text{N}$ ) in southern Italy. Fig. 17a shows disaggregation for PGA hazard at  $T_r=50\text{ yr}$ , while that for  $S_a(1\text{ s})$  and  $T_r=475\text{ yr}$  is reported in Fig. 17b. Both disaggregations have two significant modes (it will be discussed in the next sections how dominant earthquakes change with the structural period and with return period, at this stage, however, it is worthwhile to anticipate that bimodal cases are more easily available for  $S_a(1\text{ s})$  than for PGA); PDF for PGA provides first and second modal values in terms of  $R$ ,  $M$  and  $\varepsilon$  equal to  $\{35.5\text{ km}, 5.8, 0.5\}$  and  $\{125.5\text{ km}, 7.3, 1.0\}$ , respectively. The first and the second DE for  $S_a(1\text{ s})$  are  $\{132.5\text{ km}, 7.3, 1.0\}$  and

$\{35.5\text{ km}, 6.7, 0.5\}$ , respectively.<sup>8</sup> Closer zones to the site are 924, 925, 926 and 927. Zone 925 is the closest one and it determines the first DE. Zones 924 and 926 have approximately the same distance to the site, but zone 924 has higher seismicity in terms of  $M_{max}$  and  $v$  (see Table 1). Zone 927 is slightly more distant, but its seismic parameters are significantly higher than those associated to all the other zones considered here. In fact, the maximum

<sup>8</sup> Looking at Fig. 17b, it seems the first DE is that corresponding to the second mode. This is an effect of marginalization with respect to  $\varepsilon$  required to display an otherwise four-dimensional PDF on which the modes are actually identified as discussed earlier.

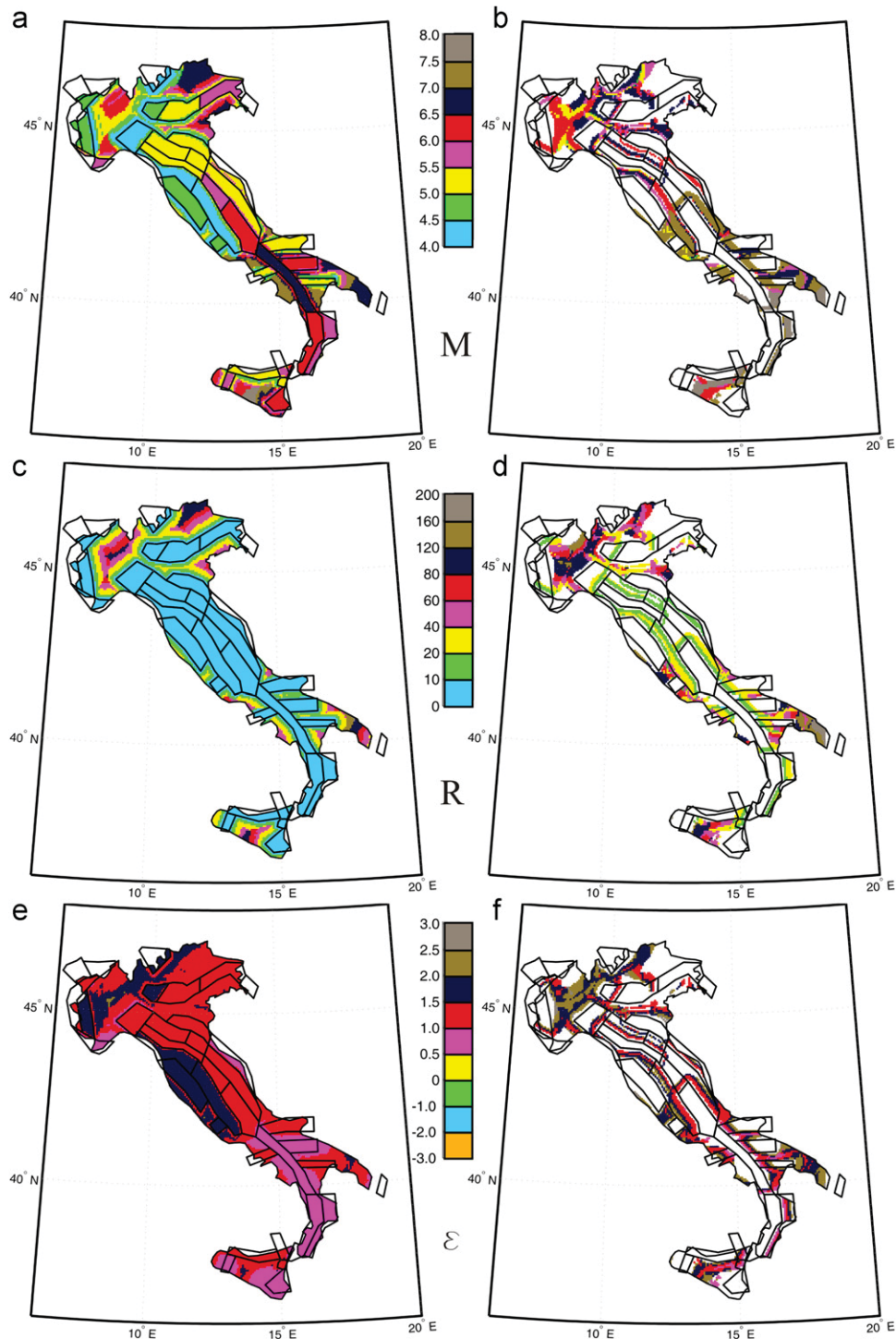


Fig. 10. First (left) and second (right) modal values for PGA and  $T_r=2475$  yr.

magnitude is 7.3 and  $v$  is almost twice of the maximum among other zones. Zone 927 is the cause of a relevant second DE.

For the same reasons behind a bimodal PDF, it is possible that a site has even more DEs. An example is Ancona (13.506°E, 43.589°N) for which  $T_r$  equal to 50 yr is considered (Fig. 18).  $S_a(1\text{ s})$  hazard disaggregation shows three modes: the first two modes in terms of  $R$ ,  $M$  and  $\varepsilon$  are {7.5 km, 5.0, 0.5} and {33.5 km, 6.2, 0.5}.

Marginalization on  $\varepsilon$ , proximity of the two modal values and bins representation make the two modes coincident in the plot.

A third significant mode corresponds to  $R$  and  $M$  equal to 110 km and 6.8, respectively. This indicates that multiple zones give comparable contribution to hazard. In fact, for this particular case zones 917 and 918 determine the first two modes (the first zone being closer and the second with slightly higher seismicity), while the more distant zone 923 has a strong seismicity and a non-negligible influence on the hazard of the site (third mode).

Because the contribution of the third mode, if any, is expected to be minor, this study is focused on the first two DEs.

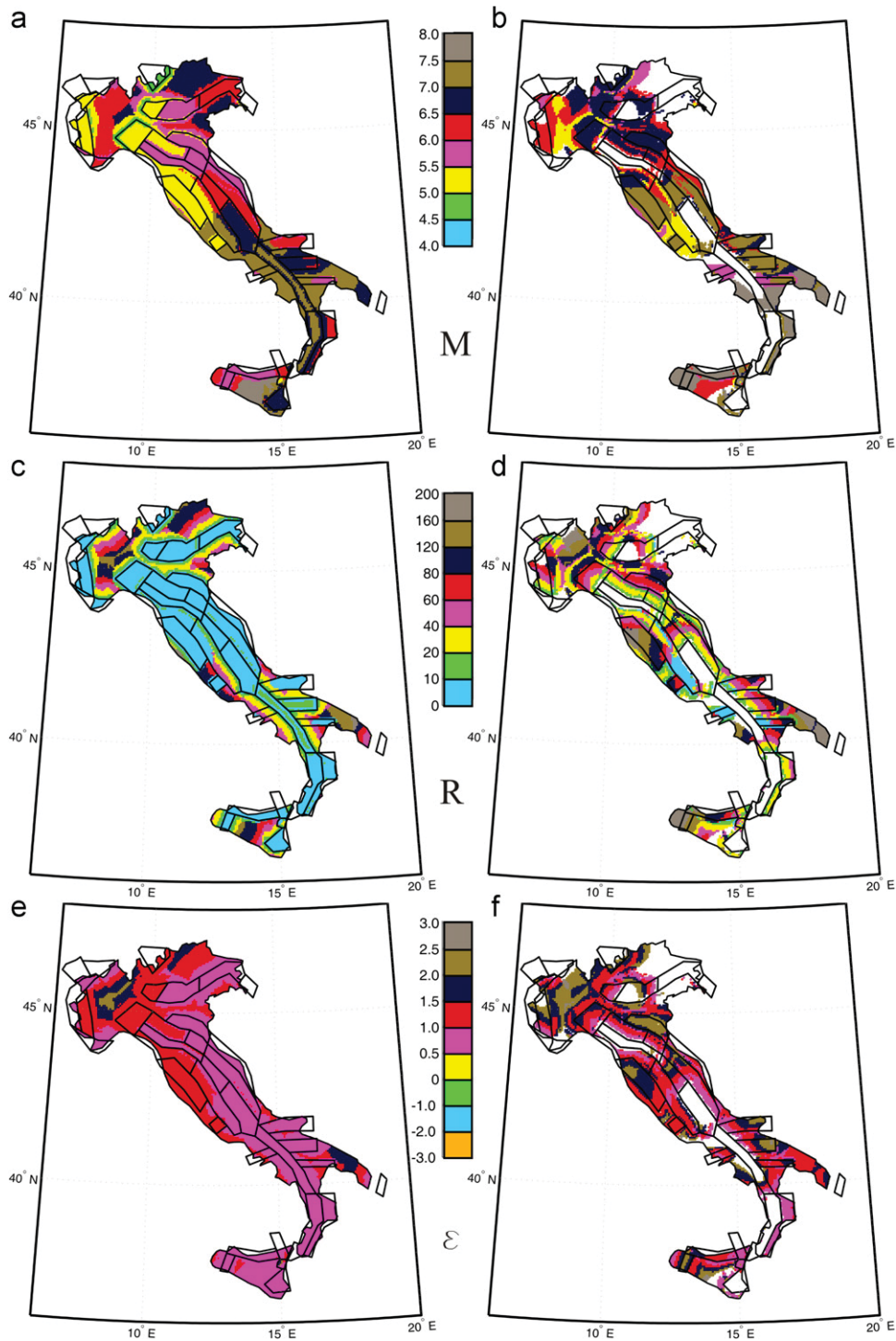


Fig. 11. First (left) and second (right) modal values of  $\varepsilon$  for  $S_a(1\text{ s})$  and  $T_r=2475\text{ yr}$ .

#### 4.1. Effect of structural characteristics on the number and significance of DEs

Maps and examples above indicate that disaggregation results can change significantly with the considered structural period the spectral ordinate refers to. This conclusion was anticipated looking at DE maps and it is also shown for the specific site of Viterbo; see Figs. 14a and c and 15a and c. The examples demonstrate that unimodal disaggregation results for PGA may become clearly bimodal for  $S_a(1\text{ s})$  with a higher magnitude and distance contribution to hazard. This is because of the GMPE. Indeed, for a

fixed site and return period, variations of dominating earthquakes for different spectral ordinates can only depend on the used prediction equation (see also Section 5). In particular, high frequency waves are attenuated faster with distance and therefore it is expected that spectral ordinates associated to longer periods (1 s in this case) are more affected by distant events with respect to PGA. In other words, distant zones, with negligible influence on PGA hazard, can show non-negligible effects on the  $S_a(1\text{ s})$  hazard at the same site. As a consequence, design scenarios based on PGA disaggregation can be potentially misleading for moderate-to-long fundamental periods as also discussed in [9].

5. Scenarios and return periods

An interesting result, which may not be inferred directly from DE maps, is that for most of the sites featuring more than one mode, increasing the return period of the acceleration being disaggregated, the contribution of the first mode (the close-moderate earthquake) increases with respect to the second mode. See, for example, San Severo (15.377°E, 41.687°N), whose disaggregation results for return periods equal to 50 and 2475 yr are reported in Fig. 19 for both spectral ordinates considered. The influence of return period on the significance of the first mode is visible for both PGA and Sa(1 s), although for PGA the effect is less evident because, as already discussed, more distant zones have lower influence on hazard with respect to Sa(1 s) hazard.

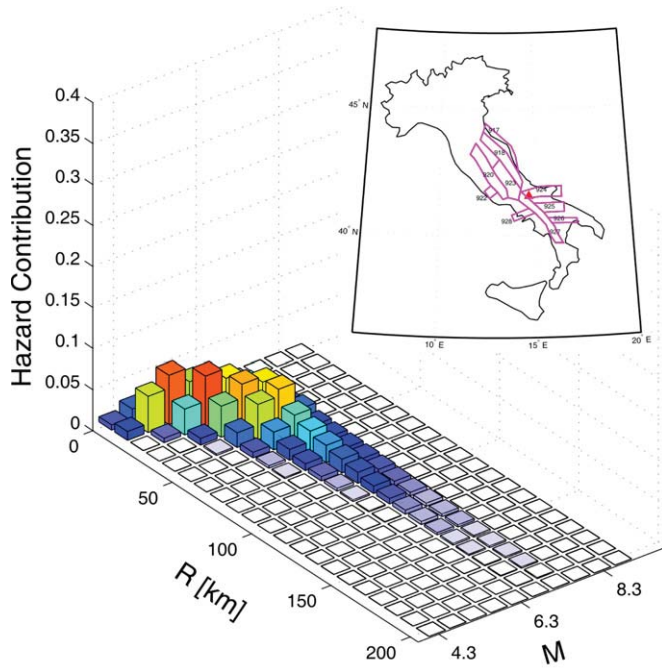


Fig. 12. Disaggregation Sa(1 s) hazard with Tr=50 yr in Campobasso.

In order to demonstrate this trend of DEs' contributions to hazard (HC) with respect to Tr, it may be useful to consider an extremely simple ideal case of a site affected by two source zones, Z<sub>1</sub> and Z<sub>2</sub>, generating individual (characteristic) earthquakes {M<sub>1</sub>,R<sub>1</sub>} and {M<sub>2</sub>,R<sub>2</sub>}:

$$HC_{Z_1} = \frac{v_{Z_1} \cdot f(IM > IM_0 | M_1, R_1)}{\lambda_{IM_0}} \tag{2}$$

$$HC_{Z_2} = \frac{v_{Z_2} \cdot f(IM > IM_0 | M_2, R_2)}{\lambda_{IM_0}} \tag{3}$$

where  $\lambda_{IM_0}$  is a marginal probability and it does not depend on the considered zone;  $v_z$  is the rate of occurrence of earthquakes for the two zones and  $f(IM > IM_0 | m, r)$  depends on the GMPE. Comparison of hazard contribution of the zones can be investigated via the ratio given in the following:

$$\frac{HC_{Z_1}}{HC_{Z_2}} = \frac{f(IM > IM_0 | M_1, R_1) v_{Z_1}}{f(IM > IM_0 | M_2, R_2) v_{Z_2}} \tag{4}$$

For a given return period, the zone with the higher product of activity rate and GMPE terms provides the higher contribution to hazard. Increasing Tr,  $IM_0$  increases and the ratio of probabilities given by GMPE determines all the relative variations of contributions.

An illustrative numerical example may be given considering the scheme of site and zones sketched in Fig. 20a. Considering the Ambraseys et al. [14] GMPE, if M<sub>1</sub> and M<sub>2</sub> are assigned equal to 5 and 6.5 and using R<sub>1</sub> and R<sub>2</sub> as average distances of the two zones from the considered site (5 and 135 km, respectively), the ratio of HC (Fig. 20a) has a positive slope indicating that the contribution of Z<sub>1</sub> increases with the threshold (i.e.,  $IM_0$ ), and therefore increases if the return period is increased.

The reason for that is plotted in Fig. 20b. In fact, the GMPE provides a normal distribution of log(Sa) with a constant standard deviation with respect to M. It can be observed that by increasing  $IM_0$  the exceedance probability decreases more rapidly for Z<sub>2</sub> with respect to Z<sub>1</sub>, which explains the trend of Fig. 20a. These conclusions are confirmed by disaggregation results for Tr=50 and 2475 yr reported in Fig. 21a and b where it is shown that the site can be considered as bimodal for Tr=50 yr and unimodal for Tr=2475 yr.

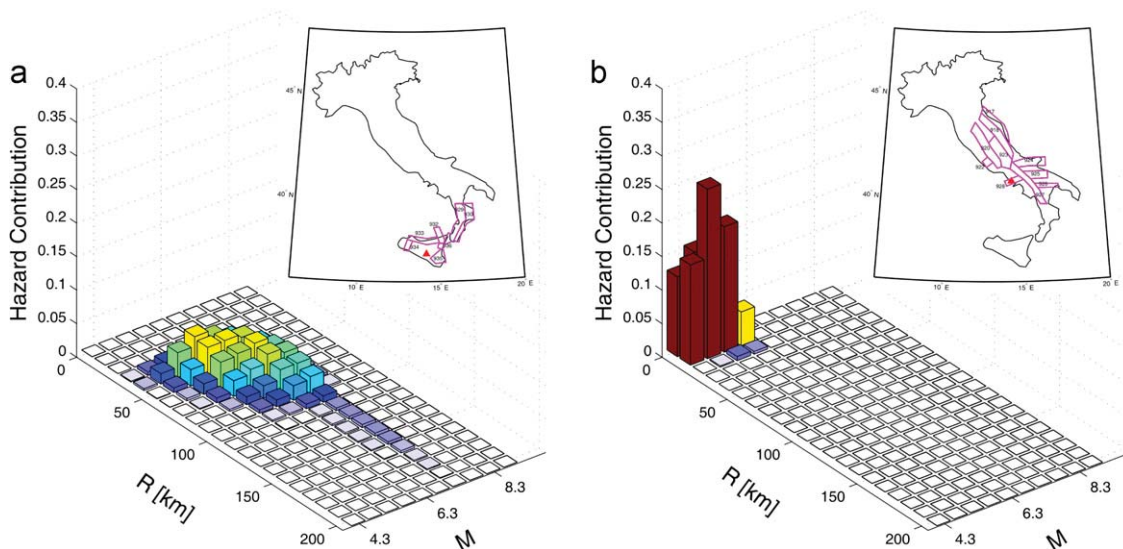


Fig. 13. Cases of relevant (a) and negligible (b) second mode hazard contribution.

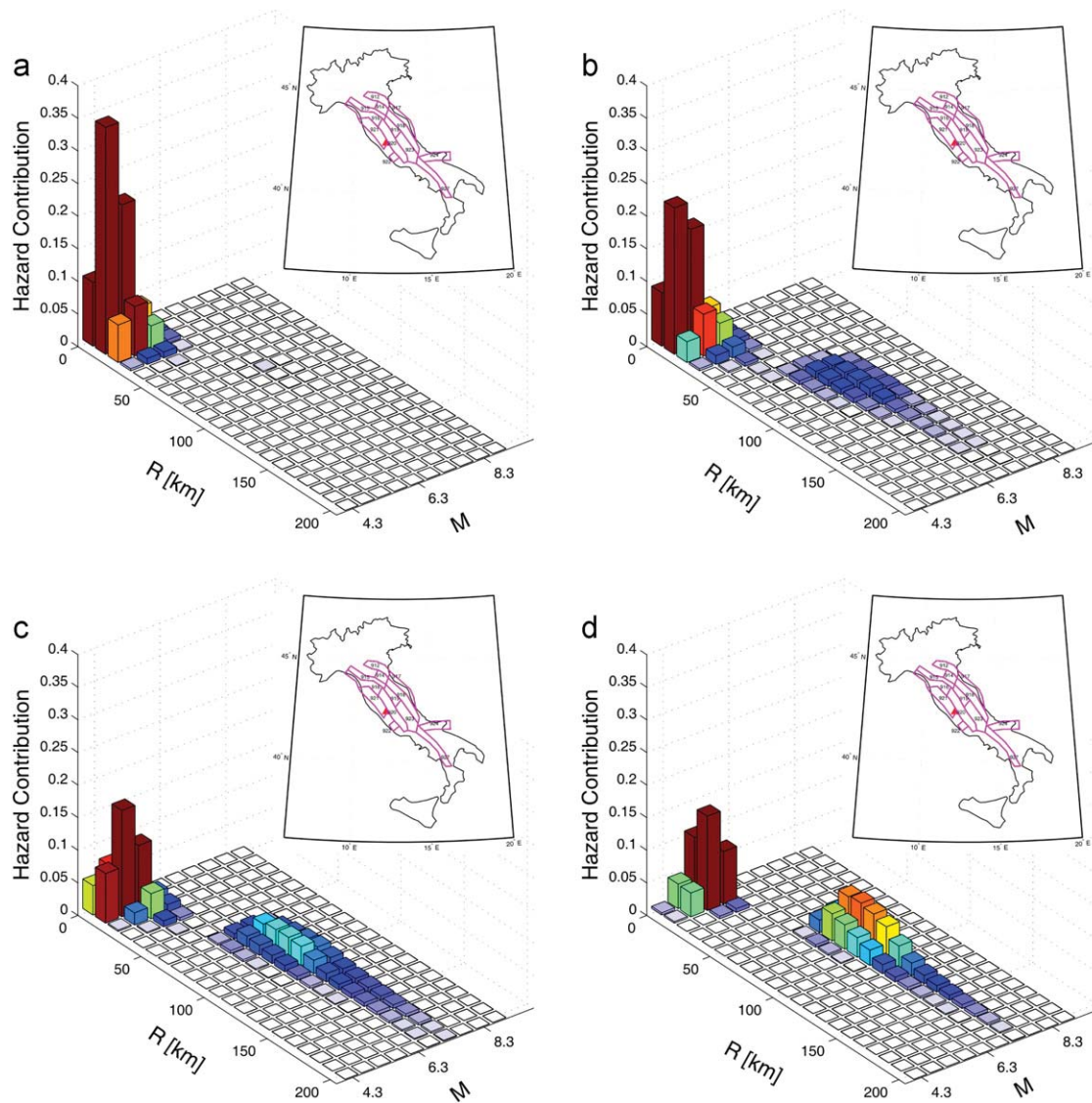


Fig. 14. Disaggregation for Viterbo and  $T_r=50$  yr: PGA (a),  $T=0.5$  s (b),  $T=1$  s (c) and  $T=2$  s (d).

These conclusions<sup>9</sup> are confirmed by disaggregation results for  $T_r=50$  and 2475 yr reported in Fig. 21a and b where it is shown that the site can be considered as bimodal for  $T_r=50$  and unimodal for  $T_r=2475$  yr. For example in the figures it is assumed that characteristic magnitude for the two zones and epicenters is uniformly distributed within these.

Finally, it is to note that an alternate case can occur when the magnitudes and distances associated to the closer zone produce average  $IMs$  lower than that due to the more distant zone. In fact, the hazard contribution that becomes negligible for higher  $T_r$  is that of the closer zone and the second scenario results of increasing importance. Frosinone (13.336°E, 41.639°N) is one of these cases as depicted in Fig. 22a and b.

<sup>9</sup> It is important to underline that earthquake occurrence rates of the zones have influence on the determination of the hazard values. If the zone with higher average  $S_a(1\text{ s})$  ( $Z_1$  in this case) has also a higher  $\nu$  rate, the influence of the second zone is practically negligible also for low  $T_r$  (so disaggregation results do not change significantly with  $T_r$ ). For presentation purposes, in the example  $\nu$  rate associated to  $Z_1$  is lower than that associated to  $Z_2$  (0.08 and 0.65, respectively).

## 6. Practice-ready engineering applications

### 6.1. Ground motion record selection for seismic structural analysis

Design may aid ground motion record selection for dynamic analysis of structures. Indeed, results of the study herein presented were included in the latest release of REXEL, a freeware software available at <http://www.relus.it/index.php?lang=en>, which searches for suites of waveforms, currently from the European Strong Motion Database and the Italian ACcelerometric Archive, compatible on average to various types of code-based or user defined spectra [20]. In fact, the suites of records that REXEL searches for are compatible to the reference (i.e., target) spectra complying with European code provisions, but selection criteria also reflect some research findings relevant for seismic structural assessment. In particular, REXEL 3.1 (beta) enables the selection of spectrum-matching records corresponding to a given range of, PGA, peak ground velocity (PGV), *Cosenza and Manfredi index* ( $I_D$ ) [21], *Arias Intensity*, and most importantly,  $M$  and  $R$ .

Because of implementation of these results in REXEL, choosing an Italian site and a return period (function of destination of the considered structure according to the Italian code), the software

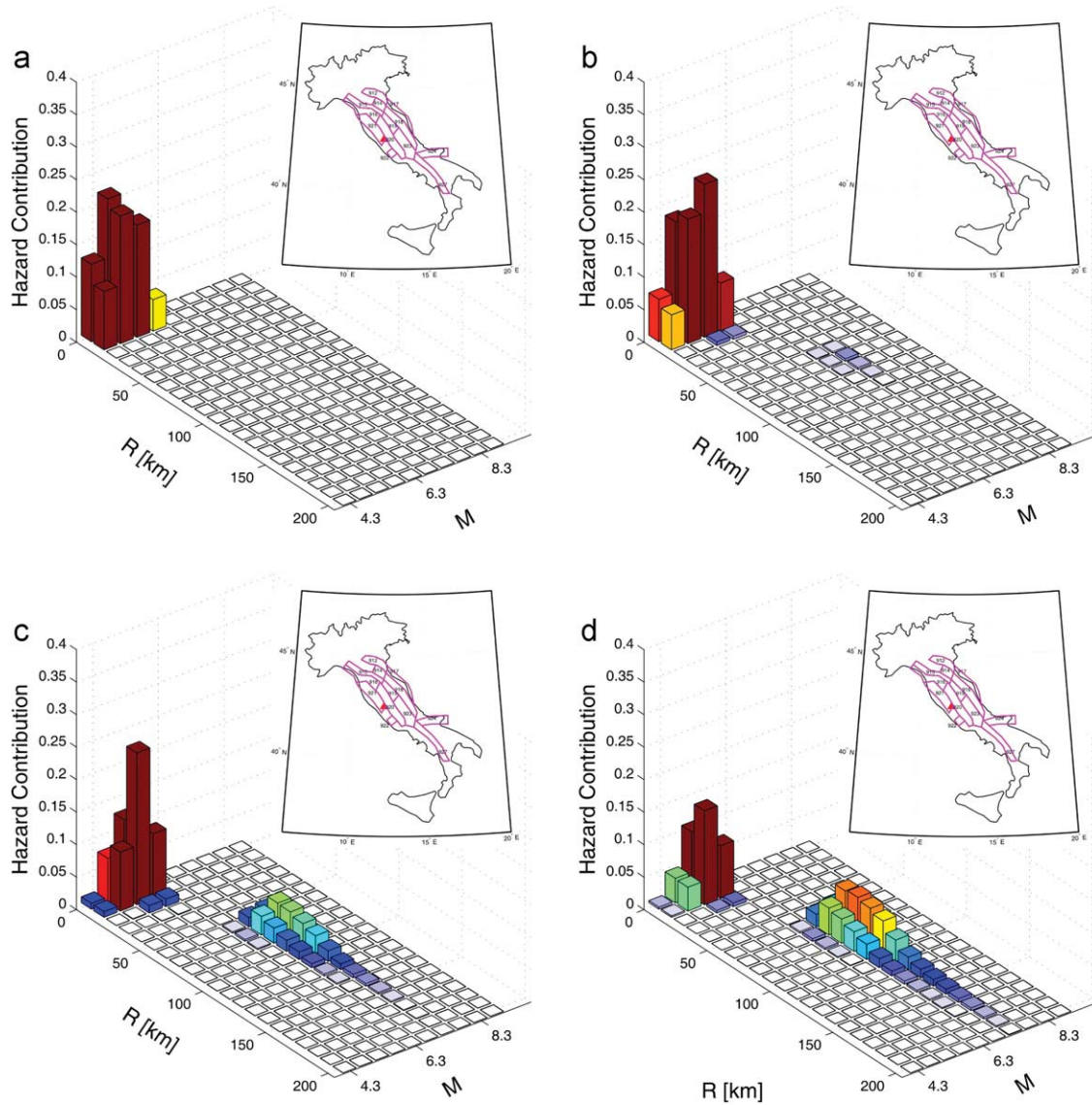


Fig. 15. Disaggregation for Viterbo and  $T_r=2475$  yr: PGA (a),  $T=0.5$  s (b),  $T=1$  s (c) and  $T=2$  s (d).

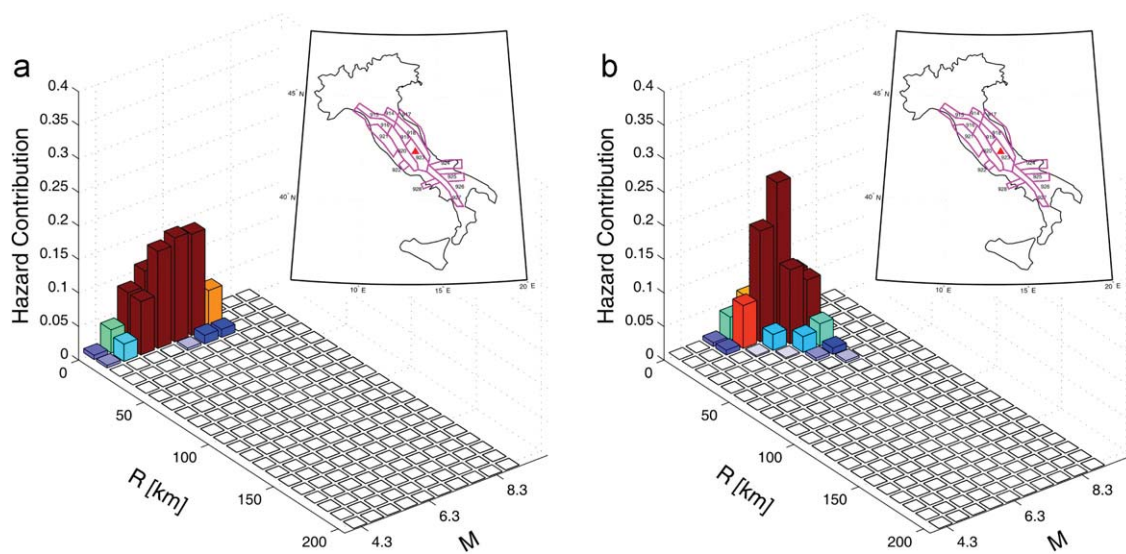


Fig. 16. Disaggregation results for L'Aquila,  $T_r=975$  yr, PGA (a) and 1 s (b).

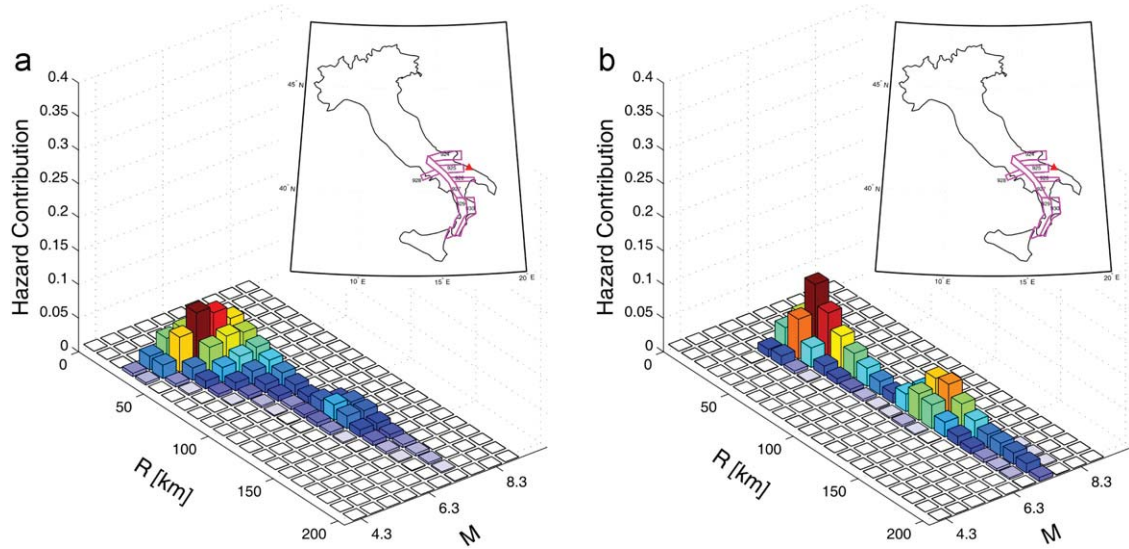


Fig. 17. Disaggregation results for Bari,  $T_r=50$  yr, PGA (a) and  $T_r=475$  yr,  $S_a(1\text{ s})$  (b).

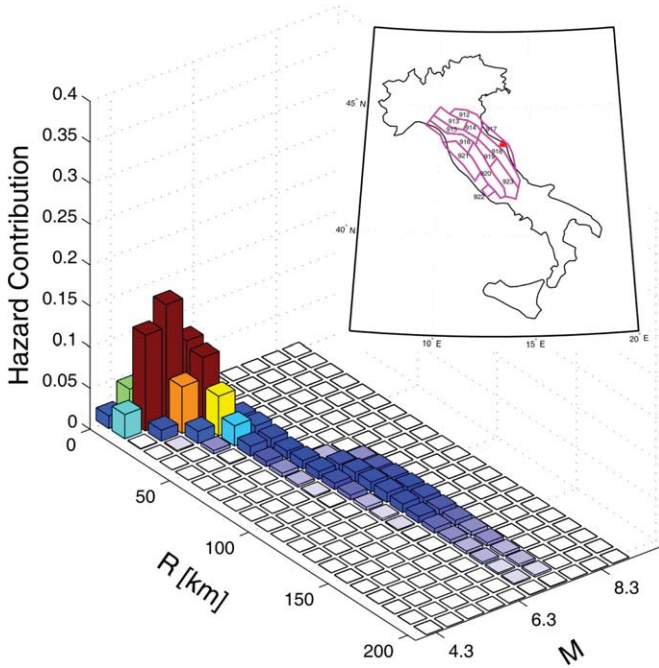


Fig. 18. Disaggregation results for Ancona,  $S_a(1\text{ s})$  and  $T_r=50$  yr.

provides tridimensional disaggregation PDFs related to PGA or  $S_a(1\text{ s})$  hazard at the closest of the four return periods computed herein. Suggesting to the user the DEs to be considered as preliminary criterion for record selection, it is possible to force REXEL to search for spectrum-matching records within the  $M$  and  $R$  bins most contributing (i.e., consistent) to the hazard the target spectrum refers to (Fig. 23).

### 6.2. Conditional hazard

Another possible use of design earthquakes is simplified vector-valued seismic hazard analysis [22]. Vectors of  $IM$  are currently under investigation by earthquake engineering research as they can improve estimation of structural response. An example of vector-valued  $IM$  may be PGA and  $I_D$ , which is the ratio of the integral of the acceleration squared to the PGA and peak ground velocity, PGV, Eq. (5).  $I_D$  is a measure related with the

cyclic content of ground motion. In fact, acceleration-based  $IM$ s (e.g., PGA or spectral ordinates) have been shown to be important in the assessment of displacement structural response of buildings, but there are cases in which the cumulative damage potential of the earthquake is also of concern and therefore parameters such as  $I_D$  may be relevant, although with a secondary role with respect to acceleration:

$$I_D = \frac{1}{PGA \cdot PGV} \int_0^{t_E} a^2(t) dt \quad (5)$$

While computing hazard analysis for vectors of  $IM$  is demanding, an easy yet hazard-consistent way of including secondary  $IM$ s in record selection is represented by the *conditional hazard maps* [23], i.e., maps of secondary ground motion intensity measures conditional, in a probabilistic sense, to the design hazard for the primary parameter for which a hazard map is often already available by national authorities.

Conditional hazard consists of computing probabilistic distribution for the secondary  $IM$  conditional to the design value of the primary  $IM$ . This requires a measure of correlation of the two  $IM$ s (e.g., [24]), and design earthquakes from disaggregation of hazard for the primary  $IM$ , to be available. In fact, it is possible to prove that under some hypotheses, the distribution of the logs of  $I_D$  conditional to the log of PGA ( $\log_{10} PGA = z$ ) is Gaussian with mean ( $\mu_{\log_{10} I_D | \log_{10} PGA}$ ) and standard deviation ( $\sigma_{\log_{10} I_D | \log_{10} PGA}$ ), which may be approximated by Eq. (6). Mean and standard deviation are a function of (i) the average and standard deviation ( $\mu_{\log_{10} I_D}; \sigma_{\log_{10} I_D}$ ) from the GMPE for  $I_D$ ; (ii) the correlation coefficient between the logs of PGA and  $I_D$  ( $\rho$ ) and (iii) the average and standard deviation ( $\mu_{\log_{10} PGA | M, R}; \sigma_{\log_{10} PGA}$ ) from the PGA GMPE. Because the conditional distribution of the logs of  $I_D$  to the logs of PGA depends on the  $I_D$  attenuation and from the PGA attenuation, it also depends on magnitude and distance, e.g., the design earthquakes  $\{M^*, R^*\}$ .

$$\begin{aligned} \mu_{\log_{10} I_D | \log_{10} PGA} &\approx \mu_{\log_{10} I_D | M^*, R^*} + \rho \cdot \sigma_{\log_{10} I_D} \frac{z - \mu_{\log_{10} PGA | M^*, R^*}}{\sigma_{\log_{10} PGA}} \\ \sigma_{\log_{10} I_D | \log_{10} PGA} &= \sigma_{\log_{10} I_D} \sqrt{1 - \rho^2} \end{aligned} \quad (6)$$

With this very simple relationship and using first modal DEs discussed in this work, conditional hazard maps of  $I_D$  can be easily produced for all the Italian sites. An example is reported in Fig. 24

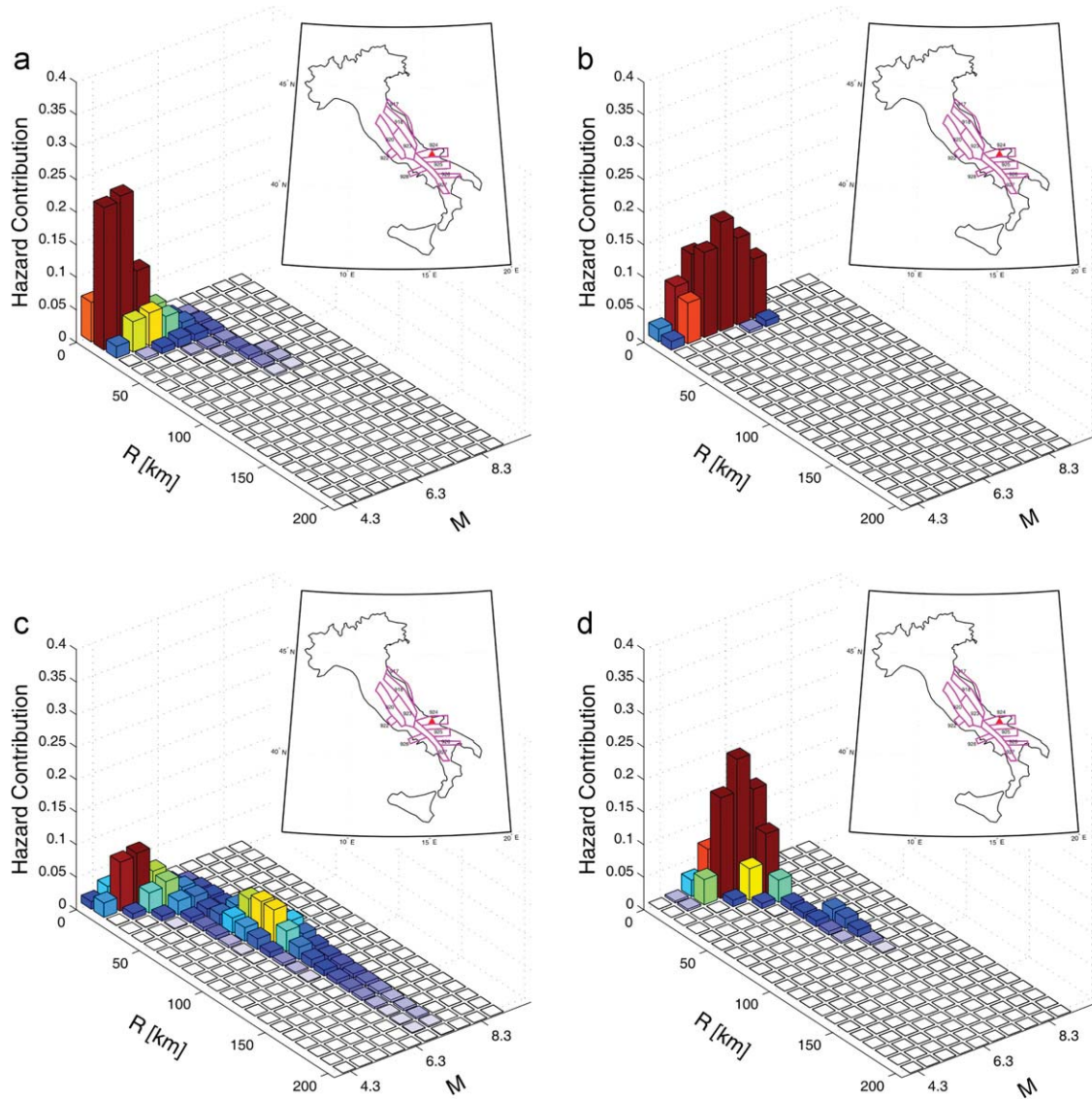


Fig. 19. Disaggregation results for San Severo at PGA for  $T_r=50$  yr (a) and 2475 yr (b) and at  $S_a(1\text{ s})$  for  $T_r=50$  yr (c) and 2475 yr (d).

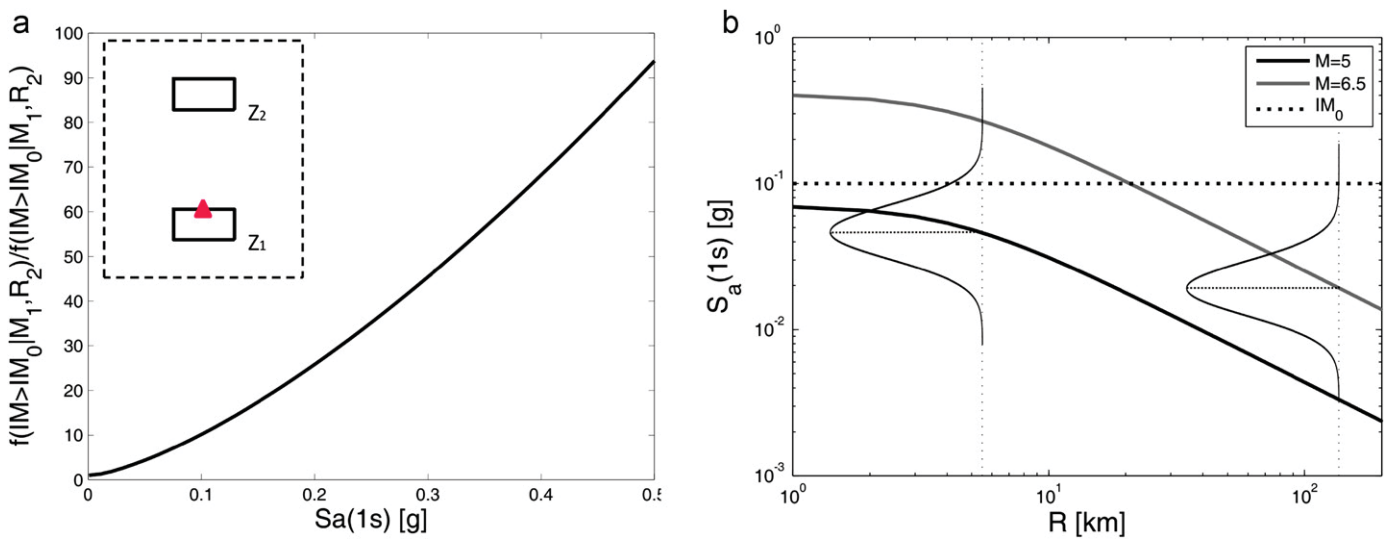


Fig. 20.  $S_a(T=1\text{ s})$  predicted by Ambraseys et al. [14] GMPE for fixed magnitude values (a) and ratio of CCDFs referred to  $Z_1$  and  $Z_2$ .

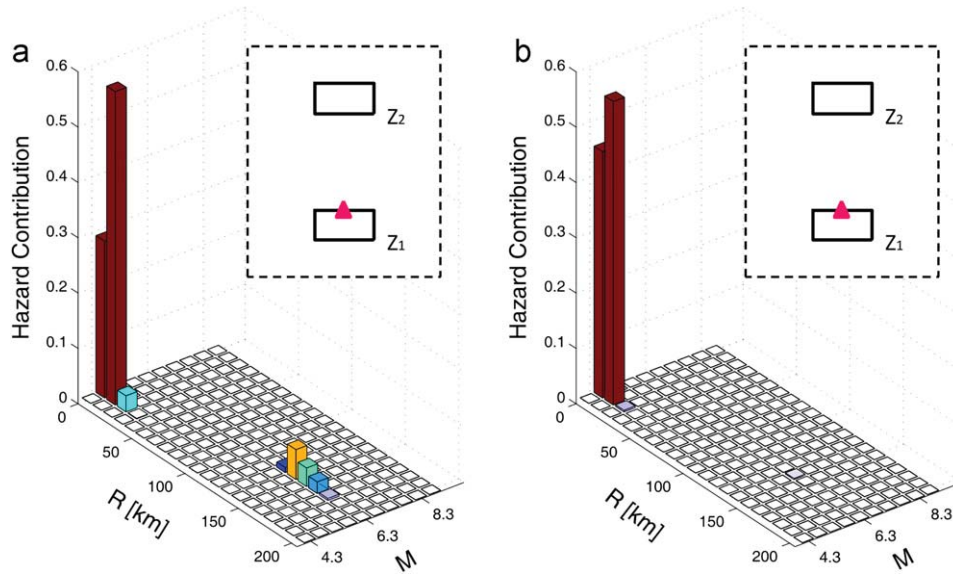


Fig. 21. Disaggregation results for  $S_a(1\text{ s})$  referring to  $T_r=50$  yr (a) and 2475 yr (b).

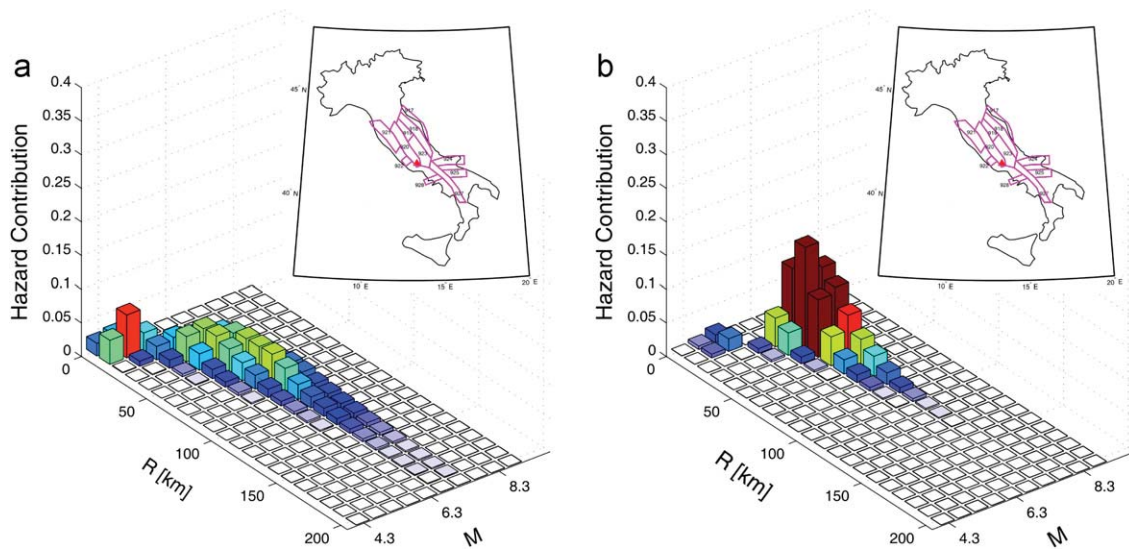


Fig. 22. Disaggregation results for Frosinone at  $S_a(1\text{ s})$  for  $T_r=50$  yr (a) and 2475 yr (b).

where two percentiles of the  $I_D$  PDF conditional to PGA with a  $T_r=475$  yr are shown.

Conditional hazard (which may be virtually extended to any pair of  $IMs$ ) is also implemented in REXEL and may be used as an additional criterion for record selection.

## 7. Conclusions

Referring to geometric modeling of seismic source zones adopted to produce Italian hazard data to which the building code is based on, and to activity parameters from literature, design scenarios were investigated in this study focusing on practical engineering use. Two different spectral periods equal to 0 s (PGA) and 1 s and four different return periods (50, 475, 975 and 2475 yr) were considered for hazard and disaggregation analyses.

Maps of first and second modal values of distance, magnitude and  $\epsilon$  were shown as synthetic representation of design earthquakes.

Moreover, extended disaggregation results for several sites were analyzed to demonstrate some general findings related to the given maps: (i) the first mode corresponds to an earthquake caused by the closer source (or the source the site is enclosed into) and with low-to-moderate magnitude, (ii) the second mode accounts for the influence of the more distant zones usually with larger magnitude and (iii) moving from PGA to  $S_a(1\text{ s})$ , the number of sites with at least two design earthquakes increases.

It was shown that sites enclosed or close to a seismic source zone with comparatively high seismicity (with respect to other zones affecting the hazard at the site) are characterized by a unimodal disaggregation PDF and, therefore, a single design earthquake can be identified. In most of the Italian cases two design scenarios show up, and in particular conditions, three design earthquakes give non-negligible hazard contribution. Dependency of disaggregation from spectral and return periods was demonstrated and some ideal examples were shown.

Finally a discussion on possible practical applications of the results of this study was provided. First, it was described how

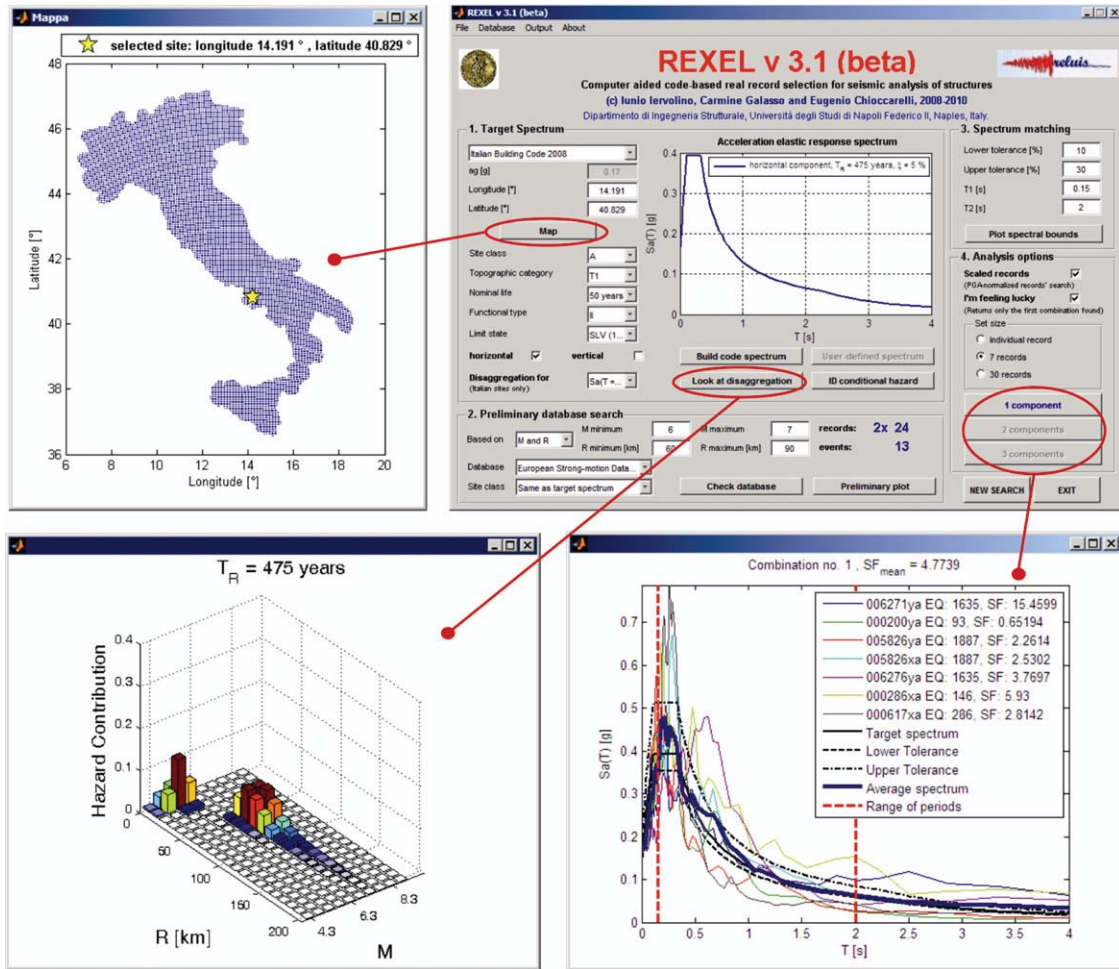


Fig. 23. REXEL software, from upper left corner clockwise: selected site, software user interface and target design spectrum for life-safety limit state according to Italian code, disaggregation for  $Sa(1\text{ s})$  in terms of  $M$  and  $R$ , selected suite of records reflecting design earthquakes and matching the target spectrum.

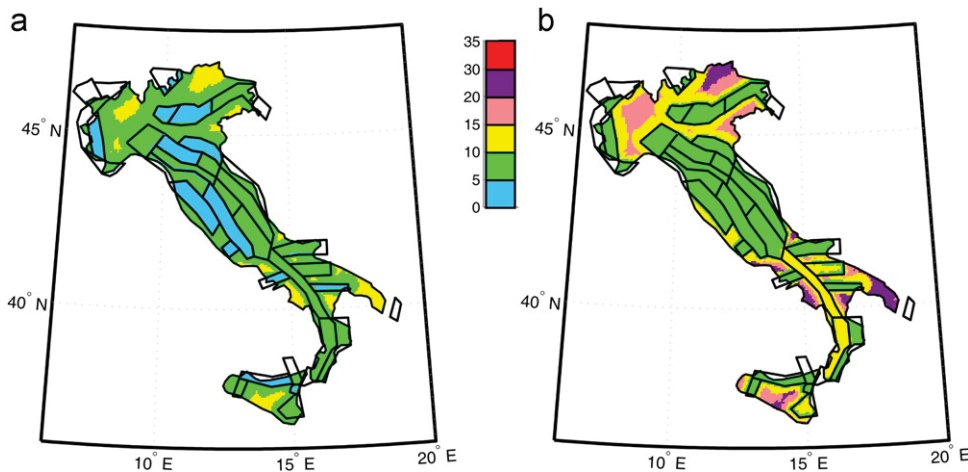


Fig. 24. Maps of  $I_D$  in terms of 50th (a) and 90th (b) percentiles conditional to PGA with a 475 yr return period and using first DEs of Fig. 6.

disaggregation distributions for all Italian sites presented in this work have been implemented in a software, REXEL, built to search for suites of spectrum-matching records. Second, the use of design earthquakes to build hazard curves for secondary intensity measures conditional to design value of acceleration was briefly reviewed.

Design earthquakes and consequent conditional hazard maps (also implemented in REXEL) seem easy to implement tools,

which can complement hazard maps to improve seismic action definitions in building codes.

**Acknowledgments**

The study presented in this paper was developed within the activities of “Rete dei Laboratori Universitari di Ingegneria

*Sismica—ReLUIS*” for the research program funded by the “*Dipartimento della Protezione Civile*” (2010–2013). The authors want to thank Racquel K. Hagen of Stanford University who proofread the article.

## References

- [1] Iervolino I, Maddaloni G, Cosenza E. Eurocode 8 compliant real record sets for seismic analysis of structures. *Journal of Earthquake Engineering* 2008;12:54–90.
- [2] Iervolino I, Maddaloni G, Cosenza E. A note on selection of time-histories for seismic analysis of bridges in Eurocode 8. *Journal of Earthquake Engineering* 2009;13:1125–52.
- [3] CEN, European Committee for Standardization TC250/SC8/(2003) Eurocode 8: Design provisions for earthquake resistance of structures, Part 1.1: general rules, seismic actions and rules for buildings, PrEN1998-1.
- [4] McGuire RK. Seismic hazard and risk analysis. Report MNO-10. Oakland, CA, USA: Earthquake Engineering Research Institute Publication; 2004.
- [5] Reiter L. Earthquake hazard analysis, issues and insights. NY: Columbia University Press; 1990.
- [6] Baker JW. The conditional mean spectrum: a tool for ground motion selection. *Journal of Structural Engineering* 2011;137:322–31.
- [7] CS.LL.PP. DM 14 gennaio 2008 Norme Tecniche per le Costruzioni. *Gazzetta Ufficiale della Repubblica Italiana*; 2008, 29 [in Italian].
- [8] Bazzurro P, Cornell CA. Disaggregation of seismic hazard. *Bulletin of the Seismological Society of America* 1999;89:501–20.
- [9] Convertito V, Iervolino I, Herrero A. Importance of mapping design earthquakes: insights for the Southern Apennines, Italy. *Bulletin of the Seismological Society of America* 2009;99:2979–91.
- [10] Bommer JJ. Earthquake actions in seismic codes: can current approaches meet the needs of PBSD? Performance based seismic design concepts and implementation. PEER Report 2004/05. Pacific Earthquake Engineering Research Center, University of California, Berkeley, US; 2004.
- [11] Meletti C, Galadini F, Valensise G, Stucchi M, Basili R, Barba S, et al. A seismic source zone model for the seismic hazard assessment of the Italian territory. *Tectonophysics* 2008;450:85–108.
- [12] Barani S, Spallarossa D, Bazzurro P. Disaggregation of probabilistic ground motion hazard in Italy. *Bulletin of the Seismological Society of America* 2009; 99:2638–61.
- [13] Barani S, Spallarossa D, Bazzurro P. Erratum to disaggregation of probabilistic ground-motion hazard in Italy. *Bulletin of the Seismological Society of America* 2010;100:3335–6.
- [14] Ambraseys NN, Simpson KA, Bommer JJ. Prediction of horizontal response spectra in Europe. *Earthquake Engineering and Structural Dynamics* 1996; 25:371–400.
- [15] Joyner WB, Boore DM. Peak horizontal acceleration and velocity from strong-motion records including records from the 1979 Imperial Valley, California, Earthquake. *Bulletin of the Seismological Society of America* 1981;71:2011–38.
- [16] di Lavoro Gruppo. Redazione della Mappa di Pericolosità Sismica Prevista dall'Ordinanza PCM 3274 del 20 Marzo 2003. Rapporto conclusivo per il Dipartimento della Protezione Civile. INGV, Milano-Roma 2004; 65 p [in Italian].
- [17] Stucchi M, Meletti C, Montaldo V, Crowley H, Calvi GM, Boschi E. Seismic hazard assessment (2003–2009) for the Italian Building Code. *Bulletin of the Seismological Society of America*, in press.
- [18] Chioccarelli E. Design earthquakes for PBEE in far-field and near-source conditions. PhD thesis. Dipartimento di Ingegneria Strutturale, Università degli Studi di Napoli Federico II, Italy; 2010. Advisors: Manfredi G, Iervolino I. Available at: <<http://www.dist.unina.it/doc/tesidott/PhD2010.Chioccarelli.pdf>>.
- [19] Iervolino I, Manfredi G. A review of ground motion record selection strategies for dynamic structural analysis. In: Bursi Oreste S, Wagg David J, editors. Modern testing techniques of mechanical and structural systems. CISM Courses and Lectures 502, Springer; 2008.
- [20] Iervolino I, Galasso C, Cosenza E. Rexel: computer aided record selection for code-based seismic structural analysis. *Bulletin of the Earthquake Engineering* 2010;8:339–62.
- [21] Manfredi G. Evaluation of seismic energy demand. *Earthquake Engineering and Structural Dynamics* 2001;30:485–99.
- [22] Bazzurro P, Cornell CA. Vector-valued probabilistic seismic hazard analysis (VPSHA). In: Proceedings of the 7th US national conference on earthquake engineering. Paper no. 61. Boston, MA; July 21–25, 2002.
- [23] Iervolino I, Giorgio M, Galasso C, Manfredi G. Conditional hazard maps for secondary intensity measures. *Bulletin of the Seismological Society of America* 2010;100:3312–9.
- [24] Baker JW, Cornell CA. Correlation of response spectral values for multi-component ground motions. *Bulletin of the Seismological Society of America* 2006;96:215–27.